UNIVERSITY OF TWENTE.

Faculty of Engineering Technology

Derivation of crack growth law from high cycle fatigue vibration testing in thermoplastic-based composites

Denny Hariadi Simanjuntak

Master of Science Thesis

January 2020

Graduation Committee:
Dr. Ir. Richard Loendersloot
Dr. Dario Di Maio
Dr. Ir. W.J.B Grouve

Master Mechanical Engineering
Faculty of Engineering Technology
University of Twente
P.O. Box 217
7500 AE Enschede
The Netherlands

Preface

Philippians 4:13, "I can do all this through Him who gives me strength". I owe everything I know today due to my personal experiences and the magical people I have aligned with, all because of God. From now on, I will always mention my guiders when celebrated for the version they helped me evolve into.

I would like to express my sincere gratitude to my supervisor, Dr. Dario Di Maio, who has guided me since day one of my thesis. I am really thankful for the kind attention and support he gave, especially during my clueless period, to make this an enjoyable journey. I would also say many thanks to Dr.Ir.Richard Loendersloot for the helpful feedback and comments. The feedback really helps me to solidify the work. I would also say thanks to my thesis committee, Dr. Ir. W.J.B Grouve. I would also say thanks to Prof. Tiedo for his input through DBM regular meeting. Thanks to Debbie for her support during my work. My gratitude to TPRC, Sebastian Wijskamp, Jagadeesh, Rick.Schrijver, GJ, Kiran, who has given me facilities through the period of manufacturing composites.

I am forever grateful to Indonesia Endowment Fund for Education that has provided my financial support for the two-year study in the Netherlands.

This journey will not be so fun without the presence of all my friends at the University of Twente. Yogesh, Dimas, Ichwan, Dayo Ladapo, Kevin, Jithin, Kiran, Rutwik, Michele Peluzzo, Henk, Mante, Robert, Michael PT, and many other friends that will make this an endless list. Thank you for sharing all the laughter and joy with me, you guys are able to keep me sane during the most stressful moments of my uni life.

Last but not least, if not due to the prayers from my family, I may not be able to reach the finish line. Thank you, Mama, Bang Dody, Debby, Dessy, Gian, and all my family for your endless support. For always believing in me and never giving up on me.

This one is for you, Bapak. "Indeed the loss of my father will always sting. But now, everything that I do is in honor of him and celebrates his life".

Denny Hariadi Simanjuntak
Twente, 22 January 2020

Summary

The global demand for carbon fiber-reinforced composite is steadily increasing over the years and will continue through foreseeable future. The market for thermoplastics alone is increasing by almost 5%. The interests of thermoplastic composites are growing due to its ability to reshape and reuse. However, in primary aircraft structures, it raises the importance of damage tolerance of this material. The most common failure mechanism in laminated composites is delamination. Therefore, the ability to predict delamination behavior is important, not only for static, but also for establishing dynamic damage tolerance criteria.

Ply-drop is one of the challenges in tapered composites due to it is the area of high-stress concentration. Hence, it is likely the point from which the crack and delamination could initiate. The structural discontinuities within the laminate produce out-of-plane stresses [1], which cause delamination of the composite structure. There are numerous experimental and analytical studies have been reported regarding various aspects of this problem. However, the study on the influence of ply-drop under fatigue behavior, especially with thermoplastic-based composites laminates, still received little attention. Moreover, there is no standard specimen for high cycle fatigue testing. ASTM D6115/ASTM D5228 only specify specimen for a quasi static load test. A novel ply-drop design has been proposed and tested to better understand the crack growth rate under fatigue tests.

This thesis started with designing and manufacturing the fit ply-drops specimen to be studied. The discovered specimens, specimen UD and specimen 0-90 are brought to vibration fatigue test. The specimen themselves are the product of iteration from the manufacturing of composite and vibration testing. The effect of high cycle fatigue is evaluated through its stiffness degradation, involving dynamics parameters, and micrograph to understand its structural performance.

The results give an understanding of structural integrity change of thermoplastic composite, which is reflected by stiffness degradation, response phase shift, and base acceleration, and resonance frequency decay caused by the crack propagation. Furthermore, the characterization of fatigue of both specimens is determined. 3D Finite Element (FE) model is carried out with the use of ANSYS-Software to simulate the real experiment to understand the involving stress, which is used to determine the strain energy release rate. The strain energy release rate that influences the delamination growth is found. Delamination growth

per fatigue cycle, da/dN, which is from the experiment is related to strain energy release rate, G from the model. At last, the ultimate aim of derivation crack growth law, which is an expression that relates delamination growth per cycle with strain energy release rate, G, is determined. The exponents of the power-law relationship can be used as a crack growth prediction tool in the case of vibration fatigue loading.

Contents

List of Figures

List of Tables

Chapter 1

Introduction

1.1 Background

Carbon fibre reinforced polymers (CFRP) are a high strength composite material, consisting of two phases of materials, carbon fibres, and polymer matrix. Carbon fibre is the major load-bearing component in polymer composites providing strength and stiffness, and the polymer matrix serves as a load distributor by uniformly transferring the applied force to the fibre. Accordingly, the polymer matrix needs to hold the carbon fibres firmly to establish an efficient load transfer, which in turn increases the mechanical properties of the polymer composites [9].

Polymer matrix in a composite material is classified into two classes, thermoplastic and thermosetting polymers, In recent years, the application of of fiber-reinforced composites is becoming more and more versatile in many applications, i.e, automative, aerospace, construction, and medical industries because of its mechanical properties and high spesific strength. As can be seen in Figure 1.1, the global demand for carbon fiber-reinforced composite is steadily increasing over the years, and will continue through foreseeable future; The market for thermoplastics alone is increasing by almost 5% over these periods. The interests of thermoplastic composites are growing due to its ability to reshape and reuse.

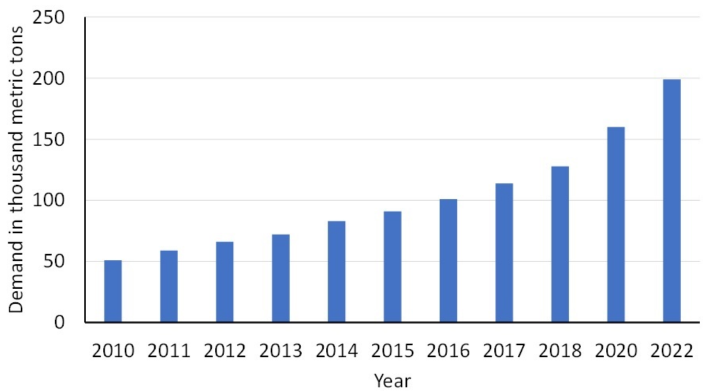

Figure 1.1: Global demand for carbon fiber reinforced plastics from 2010 to 2022 (in 1,000 metric tons) [2].

In primary aircraft structures, it raise the importance of damage tolerance of this material. The most common failure mechanism in laminated composites is delamination [10], [11]. Therefore, the ability to predict delamination behavior is important, not only for static, but also for establishing dynamic damage tolerance criteria. Boller [12] explained that the variables in a composites evaluation seem to be astronomical, but when properly understood they really are not. Each variable must be considered separately and weighed according to how it affects the service life of the composite/components. Because of the complexity of the behavior of composite materials under dynamic stress, there is a serious need for data generated according to basic principles and reported precisely.

Ply-drop is one of the challenges in tapered composites due to it is the area of high-stress concentration. Hence, it is likely the point from which the crack and delamination could initiate. The structural discontinuities within the laminate produce out-of-plane stresses [1], which cause delamination of the composite structure. Numerous experimental and analytical studies have been reported regarding various aspects of this problem. However, the study on the influence of ply-drop under fatigue condition, especially with thermoplastic-based composites laminates, still received little attention. And, currently there is no standard specimen for high cycle fatigue testing. ASTM D5228 and ASTM D6115 only specify specimen for quasi static load test.

Therefore, the purpose of this work lies in the identification of failure criteria and parameters caused by the change of the structural performance of the ply-drops thermoplastic-based composite. The work starts from designing and manufacturing the fit ply-drops specimen to be studied. Different stacking sequence, UD ply-drop, and 0-90 ply-drop are manufactured, and studied to get Ultimately, the work is then extended on the derivation of crack growth law. Through this work, the vibration fatigue test is used to generate data and to characterize delamination growth under cyclic loading. It is also understood that it is equally important to develop testing standards for characterizing delamination growth under high cyclic loading, since there is no recommended procedure for cyclic delamination characterization. Therefore this study is also aimed to be useful for enriching, and developing delamination test and specimen standards.

1.2 Thesis Project

1.2.1 Research Objective

This thesis is aimed at understanding the structural performance of ply-drops in thermoplastic based composites under fatigue condition. The failure criteria and influence of ply-drops to dynamics parameters are studied under High Cycle Fatigue (HCF) condition. The overall thesis objective is summarized in the following statement:

Derivation of crack growth law from vibration testing in thermoplastic-based composite

1.2.2 Research Questions

To achieve the research objective, several research questions are formulated:

1. What is the effect of high cycle fatigue (HCF) under these consideration as follows,
   (a) What is the effect of HCF to crack initiation and delamination in thermoplastic composite?
   (b) What is the crack propagation rate in relation to fatigue cycle?
   (c) What is the crack propagation rate for thermoplastic composite with different stacking sequence, UD Ply-drops and 0-90 Ply-drops.
2. What is the effect of damage (crack initiation and delamination) on dynamic parameters?
   (a) What is the effect of the crack to frequency, response phase, and base acceleration, and modal stiffness?
   (b) To what extent the delamination in ply-drops can captured in dynamic parameters?
3. How can a crack growth law, in particular Paris Law, for thermoplastic composite be derived?

1.2.3 Thesis outline

This thesis project aims to provide the readers the performance of ply-drops of thermoplastic composite. The approach can be divided into two main focus. The first focus is study the crack growth rate from vibration testing and to study the influence of crack to dynamic parameters. The second focus is to simulate the real experiment to understand the involving stress which is used to determine strain energy release rate (SERR). The crack is modelled using FEM (Finite Element Method). Furthermore, the energy release rate (ERR) from the model is incorporated with crack propagation rate from experimental results to construct crack growth law. Both approaches are organized in the following chapters, with the workflow illustrated in Figure 1.2.

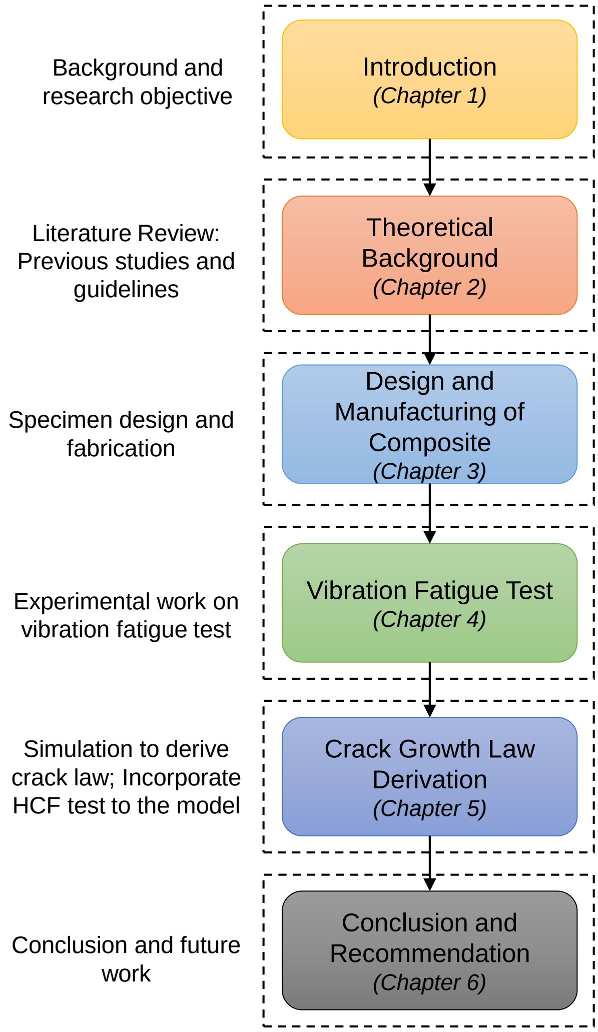

Figure 1.2: Research work flow

- Chapter 2: Theoretical Background

  This chapter describes design and manufacturing guidelines for composite laminate. Previous literature studies on fatigue and high cycle fatigue condition are discussed while the spesific research gaps are identified.

- Chapter 3: Design and Manufacturing of Composite

  This chapter covers design and manufacturing of composite laminates that in turn being used for specimens purpose. It also describes the motivation on the design and fabrication composite specimen for the test. The specimen is explained as the product of iteration from manufacturing of composite and vibration testing.

- Chapter 4: Vibration Fatigue Test

  This chapter provides experimental work on vibration fatigue test using electromagnetic shaker. Crack rate propagation is empirically derived through this experiment. The results give an understanding on structural integrity change of thermoplastic composite , which is reflected by stiffness degradation, response phase, and base acceleration, and resonance frequency de-cay caused by the crack propagation.

- Chapter 5: Crack Law Derivation

  This chapter describes the formulation of the model, which is constructed to mimic the bending mode and displacement from experiment. The strain energy release rate that influences the delamination growth is found by employing a hybrid model. Additionally, It incorporates the result from the model to the crack propagation rate from experimental results in order to construct crack law, which is a further characterization of fatigue condition of both specimens. The ultimate results, derivation of crack growth law, which is an expression that relate delamination growth per Crack cycle with strain energy release rate, G, is derived.

- Chapter 6: Conclusions and Recommendations

  The last chapter provides answers for the research questions based on the experimental results and the simulation. A set of recommendations for further improvement of this study is provided.

1.2.4 Research Contribution

Apart from the research goal, this research has contributions that can be used for other research in a wider application. More specifically, these contributions are:

- This work provides more alternative in the design and fabrication of ply-drop specimen for thermoplastic-based composite fatigue testing. Currently, there is no standard specimen for high cycle fatigue testing. ASTM D5228 and ASTM D6115 only specify specimen for quasi static load test. A novel ply-drop design has been proposed and tested to better understand the crack growth rate under fatigue tests.

- This works provides insights on the structural performance of ply-drops based-thermoplastic with different stacking sequence, UD ply-drops, and 0-90 ply-drops under fatigue.

Chapter 2

Theoretical Background

2.1 Thermoplastic Composite

Thermoplastic processing typically requires high consolidation temperatures, e.g., Polyetherketoneketone (PEKK) melting temperature is 337°C, and there is no curing chemical reaction during the consolidation process. Furthermore, thermoplastic polymers also differ from thermoset in having a significantly higher viscosity and can be amorphous or semicrystalline. The melt viscosity of thermoplastics is as high as 100 – 1000 Pa s, which is very difficult to penetrate the resin through the fibres and ensure complete wetting of the fibres [13]. Hence, thermoplastic manufacturing processes differ from traditional thermoset processes. Different processing conditions as cooling rate should be considered as a key parameter [9].

Beside the ability to reshape and reuse, thermoplastic material also posses increased impact and chemical resistance, low moisture absorption, unlimited shelf time and short processing time [9]. However, the studies on the structural performance of thermoplastic-based composites, especially, ply-drop feature under fatigue condition still received little attention. The importance of predicting the life of a ply-drop component working within safe operational conditions is of important, especially in the aerospace sector to design reliable, efficient and lightweight structures. Performance of a composite structure relies heavily on fiber orientation and lay-up sequence [9].

2.1.1 Design and Manufacturing Composite

2.1.2 Manufacturing Composite

In manufacturing composites, there are four basic steps which are wetting/ impregnation, lay-up, consolidation, and solidification. All composites manufacturing processes involve the same four steps, although they are manufactured in different ways. The methods of applying heat, pressure, and creating a desired fiber distribution, are different for different manufacturing methods. For a deeper insight into the different type of manufacturing process theme, it is recommended to refer to Mazuumdar [9]. The brief explanation of four steps can be summarized as follow,

1. Impregnation is the step where fibres and resins are mixed together to form a lamina. In this work, which involves hand lay-up process, prepregs are used. Prepreg is the already impregnated product.

2. Lay-up is the step where composites laminates are formed by placing fiber resin mixtures or prepregs at desired angles. In a prepreg lay-up process, prepregs are laid at a specific fiber orientation. This step is actually essential for the performance of a composite structure since it relies heavily on fiber orientation and lay-up sequence.

3. Consolidation is the step where it applies heat and pressure to create intimate contact between each layer of prepreg. This is an essential step to obtain a good quality laminate. Many attempts on having good laminate fails during this step.

4. Solidification is the final step where in thermoplastic is to lower the temperature to obtain a solid laminate.

Manufacturing thermoplastic has advantages and disadvantages compared to the thermoset. The advantage of manufacturing composites are relatively shorter process cycle time, it can be reshaped, and reformed with the application of heat and pressure, and easy to recycle. Meanwhile, the disadvantage is that thermoplastic requires heavy and strong tooling for processing. thermoplastic are not easy to process, and higher heat, and pressure in the processing.

Ply-Drop Design

Ply drops in composite materials are currently a relevant design consideration in many structures or components. This ply-drop feature is related to cases with varying loads throughout the structure i.e, rotor blade of a wind turbine, and wing aircraft. The ply drop introduces a stress concentration, which possibly causing a crack to form and propagate along with the layer that forms the ply drop. Ply-drops produce internal and local stress concentrations as a consequence of geometric discontinuities and shear lag [14].

Hence to avoid those mentioned problem, general design considerations for ply-drops design has been established by NASA [15]. The guidelines are as follows,

1. For the same ply drops, thicker laminates are better in resisting delamination.

2. Dropping more than one ply at the same location increases the delamination growth rate; Not more than 2 plies are dropped at once.

3. Internal ply drops are more resistant to delamination than external ply drops.

4. Whenever possible, stacking sequences should be symmetric about the mid-plane

While taking into account the established laminate guidelines, it is deemed to be necessary to keep the aim of a fit ply-drop specimen for crack study on vibration fatigue test. Due to lack of literature on the understanding of vibration fatigue thermoplastic, and standard specimen especially made for vibration testing, many attempts were made before reaching to the final specimen design. According to Cairns, the design should be made according to the following considerations [14], and recent studies [16], the guidelines for specimen to be considered are as follows,

1. The specimen should be excited at its first bending mode;
2. Ply-drops is a likely place from which the delamination could initiate;
3. Two plies are dropped in the same place to intensify the stress concentration close to the location of the maximum bending moment;
4. The plies are dropped at the outer faces where strains are high;
5. The thicker section could have a second 0° ply after the outer 0° ply to increase the strength under the clamp. However, through this work, it is found that it could be not necessary;
6. No ply-drop on the outer faces; To avoid immediate debonding.

2.2 Damage In Composite

Studies on fatigue of Fibre-reinforced composites were strongly influenced by established methods for studying metallic components. However, since the composite is an anisotropy material, it has been more complex to understand their behaviour, Therefore, despite starting from an established framework, studies have considerably modified the approach to fatigue over the years.

Dew-Hughes [17] reviewed the scattered research on fatigue of Fibre-Reinforced Plastic (FRP) by considering the effect of cyclic loading on fibres, polymers and interfaces. The finding was that fibres got damaged through the three stages of nucleation, propagation and final failure, but they themselves did not have a direct effect on the fatigue of the component. The main contribution to the fatigue damage of a composite, especially at low stresses, was due to the interface between fibres and matrix, where there was a high stress concentration.

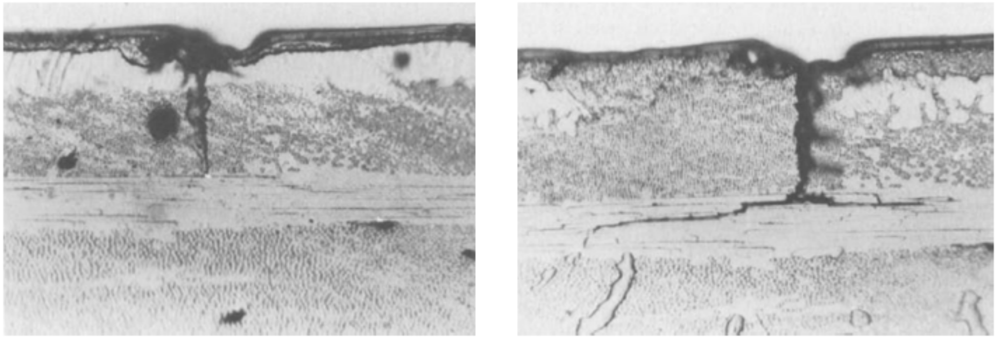

Figure 2.1: Sequence showing the growth of a crack from a 90° ply into a 0° ply in a [0; 90;45]s graphite epoxy laminate [3]

It was found that fatigue in polymeric matrix had a much different effect compared to that of fibres. Polymers suffer from thermal failure at high temperature, it dissipate heat slower than metals and tend to heat up if cyclically stressed. Despite these differences, the work done on the crack growth rate for metals was widely used to build a model for predicting crack propagation in polymers. Specifically, due to the crazing phenomenon and to the viscoelasticity of the material, the energy balance had to take into account, and its dependence on the loading frequency [7].
The interface between matrix and fibre is considered as the most crucial part for fatigue in composites. Meanwhile, fatigue strength threshold, gained from metal understanding, is of criterion importance, in order to design structures subjected to cyclic loading. The strength of the interface would avoid crack initiation below this threshold, which would prevent premature failure of composite. The limiting effect of a weak interface on the performances of the FRP, finding some debonding even at very low stress amplitudes, suggesting the impossibility of an infinite life [17]. Nevertheless, it was unclear yet, either matrix cracking or debonding, consider as failure because there was no catastrophic failure or any other observation that easily exposed the integrity of the material.

Therefore, a sequence of steps for the damage development can be summarised as follows [3], crack nucleation in off-axis plies as can be seen in the Figure 2.1 on the left. Further, crack coupling due to the interface debonding when the crack tips reach the interfaces is shown in Figure 2.1 on the right. A crack will then grow through the thickness by crack coupling and ultimately, there will be a final fracture of fibres in the direction of the load. Nevertheless, it is found that the anisotropy of FRP drives the crack in a way that is too complex to predict. In this work, it is found that the microcrack formed in the weak phase of the matrix and propagated until it was arrested by the strong phase which is fibres.

There are several possibilities for crack growth, which can be seen as follow,

1. The stress concentration is high enough to propagate the crack
2. If the critical level is not reached, the delamination will start but will arrest at a certain length and remain constant at that length [14]

3. The stress is so low that delamination never initiates within 500.000 cycles [14]. The threshold of this cycles are dependent on the characteristics of the material.

Classification of damage has also been established regarding the location of damage occurence, any damage within a single ply is named intralaminar damage which are typically fibre breakage and matrix cracking. Meanwhile any damage between different plies are called interlaminar, which is commonly known as delamination. Figure 2.2 depicts these two type damages clearly. In an accelerated vibration fatigue test conducted in this work, these two happen concurrently in a fast manner. Nevertheless, separating these damages can be of importance for characterization of ply-drop specimen.

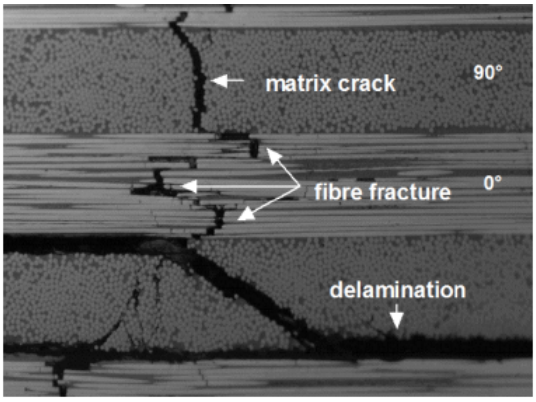

Figure 2.2: Interlaminar and Intralaminar Damages [4]

.

2.3 Fatigue Overview

2.3.1 Cyclic Loading

Cyclic loading is generally a representation of fatigue load imposed on material or component, of which typically sinusoidal waveform. Figure 2.3 shows the characteristics of the cyclic loading which consist of the quantity value of Stress (σ) against Number of Cycle (N). Strain or displacement which corresponds to the related stress also can be applied against the cycle. Stress is more convenient for homogeneous material, while the strain is more convenient for composites.

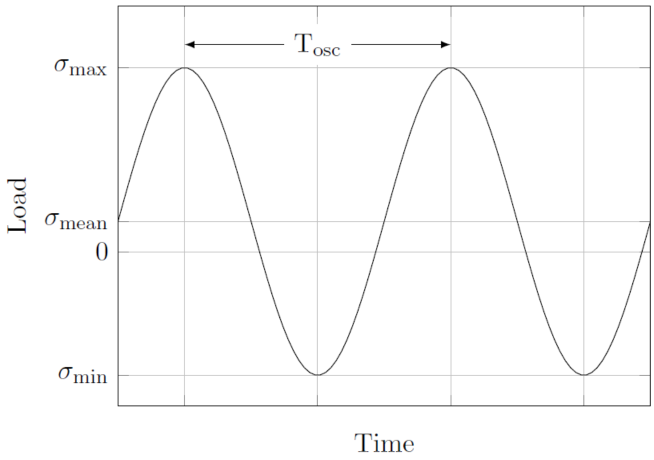

Figure 2.3: Typical sinusoidal loading conditions over time [5]

Loading conditions can be varied in frequency and magnitude value which is commonly known as loading ratio.

$$R = \frac{\sigma_{min}}{\sigma_{max}} \tag{2.1}$$

$$f = \frac{1}{\mathrm{T_{osc}}} \tag{2.2}$$

Where, R is the stress ratio. ε_{max} and ε_{min} are the maximum and minimum strain in the component respectively. T_{osc} is the period of oscillation, and f is the oscillation frequency.

The stress/strain ratio, R, gives a condition of how the material or component is subjected to loading. The loading ratio can be seen as followings,

- $0 < R < 1$ Impose tension-tension loading
- $R > 1$ Impose compression-compression
- $R < 0$ Impose tension-compression loading
- $R = -1$ Impose fully reversed loading

2.3.2 Paris Law

Regarding polymers and composite, Griffith's criterion discovered the way to the Linear Elastic Fracture Mechanics (LEFM), starting from the hypothesis that premature failure in apparently pristine components was due to microscopic flaws in the material [18]. Through his work on glass, Griffith conclude that there was a constant relationship between the stress at fracture and the square root of the notch length. It is then modified by Irwin [19], by partitioning the total energy in two contributions, The stored elastic strain energy at the crack tip and the dissipated energy to create a new surface, Creating a new surface means propagation of crack. The stored strain energy at the crack tip is released to create a new surface when it exceeds a material property called fracture toughness G_c.

The uniform stress field equation is read as follow,

$$K_{\mathrm{I}} = \sigma\sqrt{\pi a} \qquad K_{\mathrm{II}} = \sigma\sqrt{\pi a} \tag{2.3}$$

In plane stress conditions, the strain energy release rate (G) for a crack under pure mode I, or pure mode II loading is related to the stress intensity factor by,

$$\begin{aligned} G_{\mathrm{I}} &= K_{\mathrm{I}}^2 \left(\frac{1}{E}\right) \\ G_{\mathrm{II}} &= K_{\mathrm{II}}^2 \left(\frac{1}{E}\right) \end{aligned} \tag{2.4}$$

The LEFM was then incorporated in the Paris research on fatigue crack propagation [20]. Irwin's stress intensity factor, which is employed to calculate the effect of an applied stress on the local stress field ahead of the crack tip to predict the crack propagation rate under cyclic loading. Ultimately, the fundamental relationship that can relate the stable propagation with strain energy release rate can be read as follow,

$$\frac{\mathrm{d}a}{\mathrm{d}N} = C(G\mathrm{max})^m \tag{2.5}$$

It can also be related to stress intensity factor as below,

$$\frac{\mathrm{d}a}{\mathrm{d}N} = CK_{\mathrm{max}}^m \tag{2.6}$$

Where da/dN is the crack growth rate, K_{max} is the stress intensity factor, and C and n are material constants. Figure 2.4 shows where C and m are the intercept and the slope of the Paris law in a log-log plot. Fatigue crack growth in composites can be characterized by relating crack growth per cycle to the cyclic stress intensity factor range, ΔK [21]. In a number of studies, a power law has been used to relate delamination growth with cyclic strain energy release rate in composite cases.

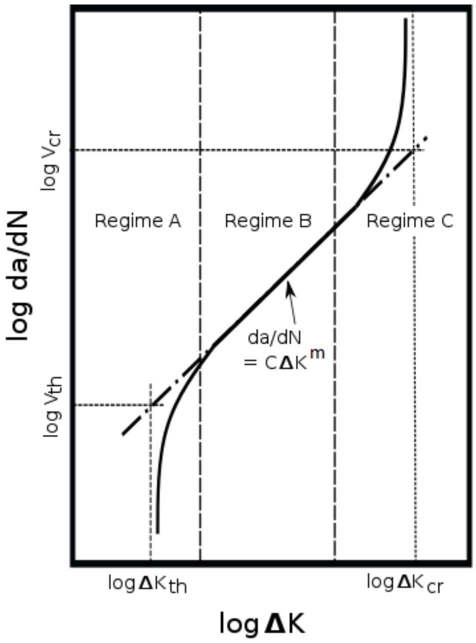

Figure 2.4: Schematic Plot of Paris's Law with C and m coefficient [6]

One of the methods for predicting the delamination growth is [22]:

$$\frac{\mathrm{d}a}{\mathrm{d}N} = C\left(\frac{\Delta G_I}{G_{Ic}} + \frac{\Delta G_{II}}{G_{IIc}}\right)^m \tag{2.7}$$

2.4 Dynamics View

Test methodologies by exploiting the resonance conditions to perform quick tests has been the theme of vibration testing for decades [23]–[28]. The simplest dynamic system is the Single Degree of Freedom (SDOF) comprising of mass, spring, and damper system described in the Figure 2.5. The mathematical expression of motion this simple system, assuming no external forces, can be read in Equation 2.8 [29].

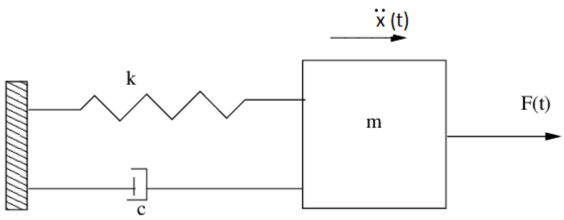

Figure 2.5: SDOF System

$$m\ddot{X} + c\dot{X} + kX = 0 \tag{2.8}$$

Where m is the mass of the SDOF system, $\dot{X}$ and $\ddot{X}$ are first and second time derivative of displacement, c is the Damping coefficient, and k is the stiffness of the spring. When Equation 2.8 solved, it reads as follows,

$$X(t) = Ae^{-\zeta\omega_n t}e^{i\omega_n' t} \tag{2.9}$$

Where A is the vibration amplitude at t = 0, ω_n is the resonance frequency, and ζ is the damping ratio. While, damping ratio and ω_n' the response frequency, read as follows,

$$\begin{aligned} \omega_n &= \sqrt{\frac{k}{m}} \\ \zeta &= \frac{c}{2\sqrt{km}} \\ \omega_n' &= \omega_n\sqrt{1-\zeta^2} \end{aligned} \tag{2.10}$$

When the external force take acting on the mass, the equation of motion read as follow,

$$m\ddot{X} + c\dot{X} + kX = F(t) \tag{2.11}$$

The transfer function can be read as follows,

$$|\alpha(\omega)| = \frac{|X|}{|F|} = \frac{1}{\sqrt{(k-\omega^2 m)^2 + (\omega c)^2}} \tag{2.12}$$

$$\phi(\omega) = \arctan\frac{\omega c}{k-\omega^2 m} \tag{2.13}$$

Vibration Testing Theory

In the framework of component testing, to characterize the material behavior by their dynamic properties is by exciting the specimens using dynamic exciter. There are several ways of excitation, i.e, contactless excitations, acoustic, electromagnetic excitation. The latter is the one to be employed in this work. Electromagnetic shakers has the ability to produce large dynamic loads by directly exciting the structure.

Figure 2.6 shows the idealization of essential components of electromagnetic shaker. It is assumed as lumped parameters to study its interaction with the structure being excited. Mass, as m_b connected to a spring k_b, and a damper, c_b that represent modal mass, axial stiffness, and damping of the base acceleration, respectively. The base is grounded, and on top of it, the excited component/specimen is respresented as an SDOF system. $X_b(t)$ is the base displacement.

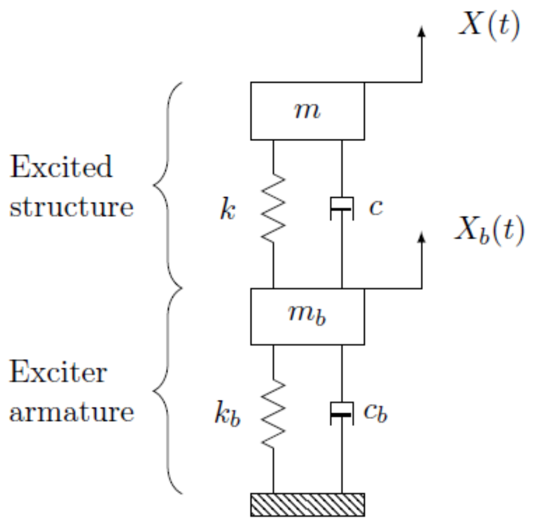

Figure 2.6: Base and Excited Structure

In this configuration, the overall idea of Equation 2.12 is still valid but the phase lag and the transmissibility in a base excitation between the base and mass displacement are read as follows

$$\varphi(\omega) = \arctan \frac{mc\omega^3}{k\left(k-\omega^2 m\right)+(\omega c)^2} \tag{2.14}$$

Through the work of Magi and Maio [7], it is shown how a measurement of the natural frequency or direct measurement of the stiffness of component due to the occurrence of damage initiation could be a poor resolution. Phase shift and base acceleration are a more sensitive approach for monitoring structural degradation, and consequently, damage initiation. Damage initiation could abruptly change the distribution of the stiffness of a component under fatigue loading conditions. Phase response is expressed in Equation 2.14. However, later on in this work, base acceleration is also found not sensitive enough to capture the period of initial crack.

$$|T(\omega)| = \frac{|X|}{|X_b|} = \frac{\sqrt{k^2+(\omega c)^2}}{\sqrt{\left(k-\omega^2 m\right)^2+(\omega c)^2}} \tag{2.15}$$

Chapter 3

Design and Manufacturing of Composite

This chapter covers design and manufacturing of composite laminates that in turn are being used for specimens purpose. The specimens are cut from the laminate. Noteworthy to mention, the specimen is the product of iteration from manufacturing of composite and vibration testing that will be covered in Chapter 4. It is found to be necessary to keep complying with the established laminate guidelines while keeping the goal of a fit ply-drops specimen for the crack study and vibration testing experiment purpose. It is discovered that ply-drops on the outer plane of the specimen with considerably high severity and loaded up to 10 million cycles do not succeed in initiating crack and producing delamination. Meanwhile, once the crack is initiated, delamination occurs in a rapid time, which is only few hundred cycles.

3.1 Material

As has been explained, composites are made of reinforcing fibers and matrix materials. Thermoplastic matrices are such as Polyether Ether Kethon (PEEK), Polyether KethoneKethone (PEKK), and Polyphenylene sulfide (PPS). The specimens are made of a 16 prepregs plies of Toray Cetex® TC1320 PEKK laminate reinforced by unidirectional carbon fibres, which is supplied by TenCate. A prepreg is a resin-impregnated fiber which is stored for later use in hand lay-up or molding operations. TC1320 is a thermoplastic composite material, with the semi-crystalline thermoplastic polymer PEKK. TC 1320 is a qualified material with outstanding mechanical performance for use in aerostructures. The material used to seed a pre-existence crack is polymide, which has smooth surface and high chemical resistance, and especially high heat resistance.

3.2 Specimen Design

The design of the testing specimen is inspired from the application of the thermoplastic composite which raise inevitable fibre discontinuities which in turn affect uncertainties of fatigue life in the composite. Ply-drops accommodate thickness variation in real application, i.e, wind turbine blade, wing aircraft.

During the earlier phase of this study, specimens with ply-drop on the outer plane of the specimen with considerably high severity and loaded up to 10 million cycles did not succeed in initiating crack and producing the expected delamination. Although it was found that there are some delaminations from unexpected spots, which suggests the flaw of the manufacturing process. The mentioned specimens were produced by an Out of Autoclave (OoA) production method. OoA is a laminate consolidation technique, which rely on vacuum pressure only. The temperature is heated in an oven. Other than these findings, there was no expected crack initiated from the edge of ply-drops. It is proven that thermoplastic based thermoplastic composites have a high resistant to fatigue. Without a pre-existence crack and ply-drops, thermoplastic composite is found to be highly resistant to vibration fatigue loading.

Considering the mentioned finding, the ply-drops were then seeded with a crack between the bottom layer of the ply-drops and its base plies. Hence, it is possible to produce delamination during the test. This work has also proven that once the crack is initiated, thermoplastic composite is prone to rapid propagation from vibration loading; it is only within few hundred thousands cycles with half of mentioned severity with laminate without pre-existence crack. Thermoplastic composites is more sensitive to crack growth under vibration loading compared to metals and ceramics [30]. Therefore, seeded crack is established by using polymide grade 25s with thickness $25\,\mu\mathrm{m}$.

After iterating of the manufactured specimens and testing the specimen to the vibration test, two stacking configurations are decided to study further. The first design is with UD lay up for both ply-drops and base plies. The second design is with a stacking sequence $(0_{plydrop}, 90_{plydrop}, (0,90)_3, (90,0)_4)$. The second design, as explained in [15], is meant to be symmetric about the mid-plane to avoid residual stress on laminate. Both specimens are shown in Figure 3.1.

From Figure 3.1, it can be seen that the final specimen design is decorated with two symmetrical length.The specimen is rectangular in shape, 254 mm length and 280 mm width. Moreover, it has 4 edge spots which can be used as a side for measuring the crack length. The 4 spots are shown in Figure 3.2. One of the pristine spots can be seen in Figure 3.3. Resin pocket can be seen clearly next to the seeded $0.25\,\mu\mathrm{m}$ polymide. Thickness variations are made by dropping plies along the length. The Difference in thickness between the thicker section and the thinner section is 0.28 mm (2 plies) , which comply with the ply-drop off guidelines [15]. However, against the guidelines, the ply-drops are put on the outer plane

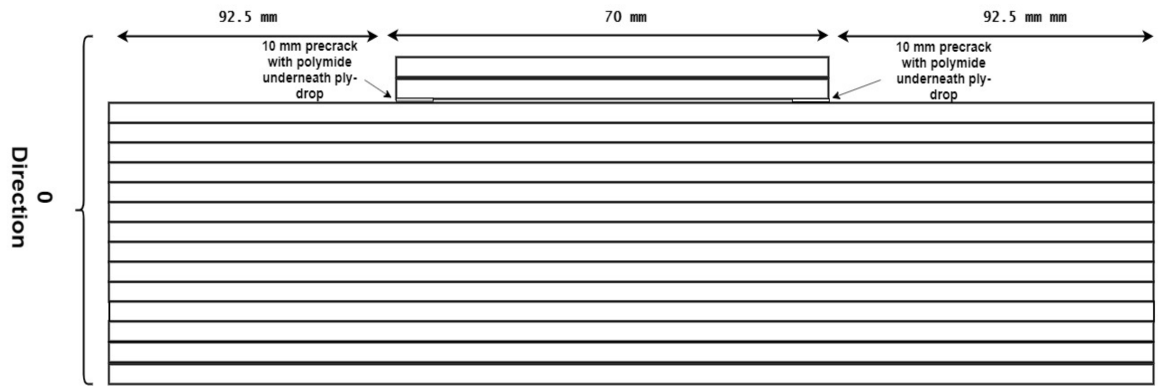

(a)

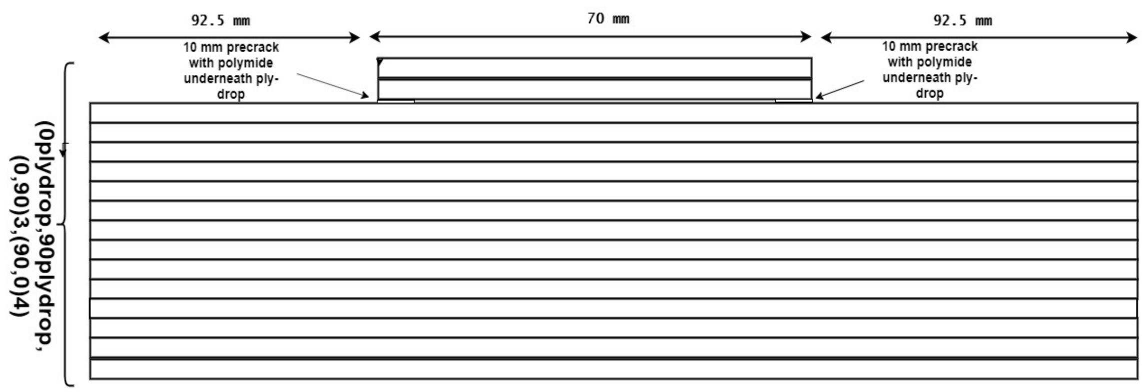

(b)

Figure 3.1: Schematic drawing of ply-drop specimen from the side (a) with UD lay up (b) as for (a) but $(0_{plydrop}, 90_{plydrop}, (0,90)_3, (90,0)_4)$ lay up

to increase the stress concentration. The purpose is to accelerate crack propagation.

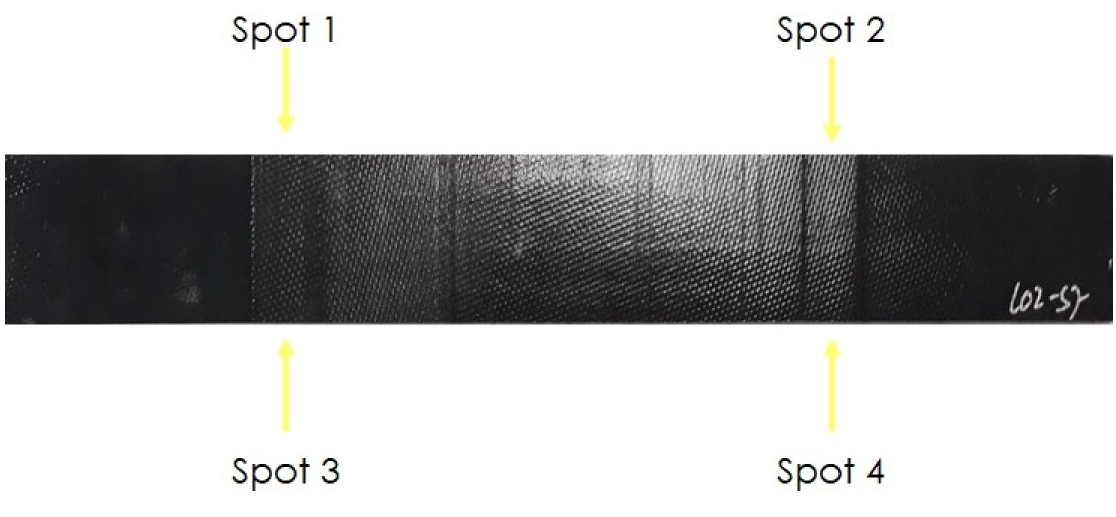

Figure 3.2: Crack spot of the specimen

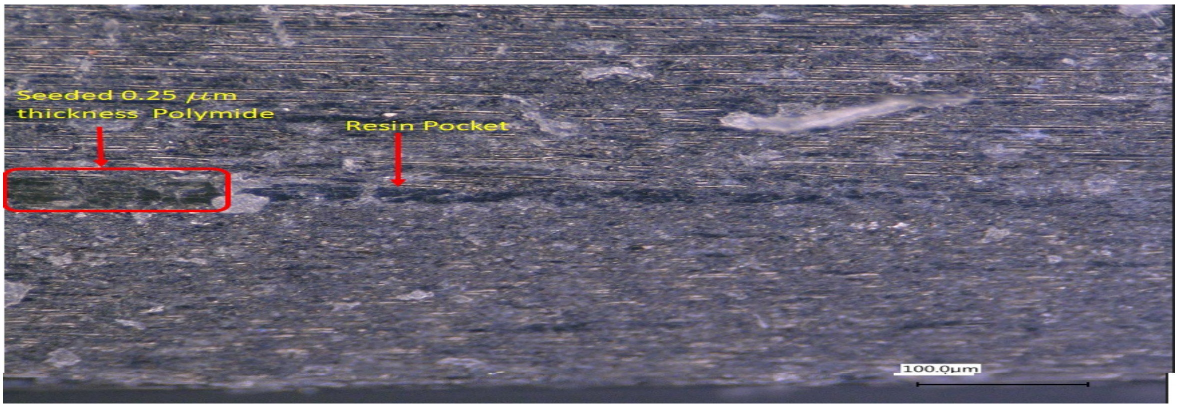

(a)

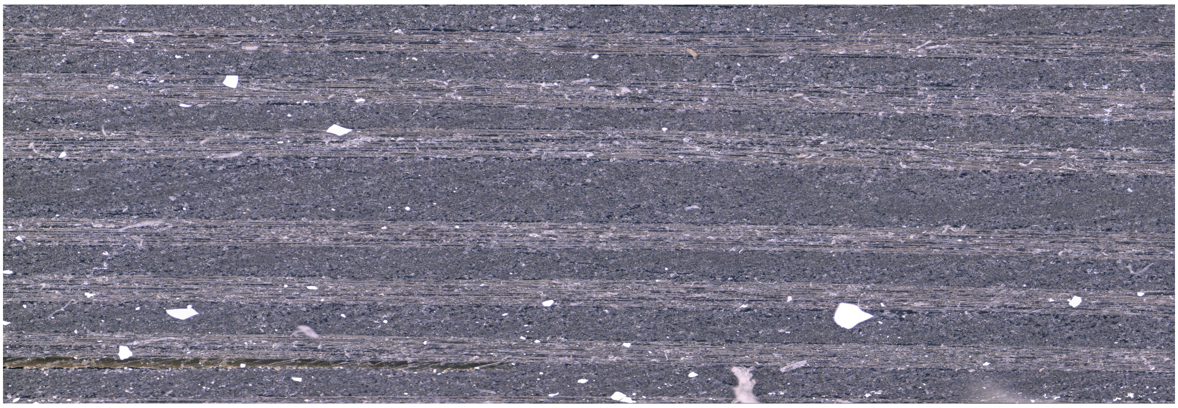

(b)

Figure 3.3: Micrograph of Pristine Composite (a) 0-0 Ply-drops (b) 0-90 Ply-drops

3.3 Manufacturing Process

As the aim of the author is to produce its own laminates for the specimens, the understanding of the manufacturing process in order to produce good quality laminates, which can give consistent mechanical properties were considered. Consolidation of thermoplastic composite using prepregs are used. A prepreg is a resin-impregnated fiber in flat form, which is stored for later use in hand lay-up or molding operations. In order to obtain consistent laminates, the process parameters, i.e, autoclave pressures, temperatures, and dwell times, of the manufacturing techniques are fixed.

The manufacturing process can be divided in three process. The first process is the prepreg lay-up process to prepare the composite stacking sequence as in designed configuration. The second process is to prepare the stack for vacuum bagging. The configuration of the vacuum bagging is shown in Figure 3.4. The third process is where the cycle of heating and curing in Autoclave take place. All these three steps are labor intensive. Labor costs are 50 to 100 times greater than filament winding, pultrusion, and other high-volume processes [9]. However, for building prototype parts and small quantity runs this type of manufacturing provides advantages over other processes.

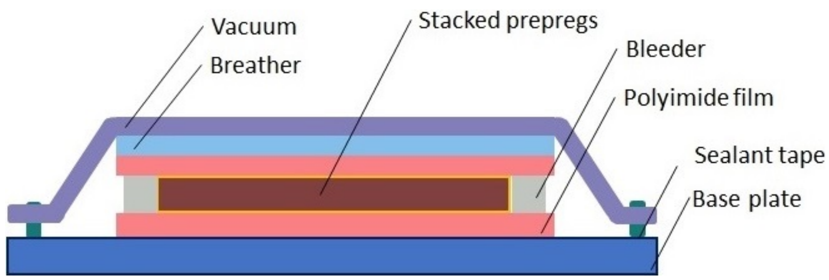

Figure 3.4: Vacuum bagging lay out for Autoclave

The first process is where the prepegs are cut, and laid one by one to build up a stack on an clean table. With the first design, the prepregs are laid on the same fibre orientation. The ply-drops are placed on the top. It is of importance to keep each plies align with its adjacent plies to achieve parallel fibres. With the second the design, the stacking sequence follows the designated sequence $[0_{plydrop}, 90_{plydrop}, (0, 90)_3, (90, 0)_4]$.

Once all the prepregs are laid in the desired sequence and fiber orientation, vacuum bagging preparations are commenced, which is the second process. Vacuum bagging started with placing the stack on a base plate (open mold) for bagging. The steps of vacuum bagging are summarized in Appendix A.1.

After stacking (lamination) and bagging, the vacuum bag is placed inside an autoclave for consolidation and curing. Autoclave maintained the desired pressure and temperature inside the chamber for processing of the laminates. Heat and pressure play an important role during consolidation process. The pressure is imposed in two ways, the bagging creates vacuum pressure. To create the vacuum, the nozzle in the bagging system is connected to the vacuum pump using a hose. The vacuum pump generates pressure until 0.1 mbar which helps in consolidation. External pressure inside the autoclave is created by injecting pressurized nitrogen. Nitrogen is used at high temperature to avoid burning or flames. Both external pressure and vacuum pressure inside the bag are expected to create sufficient pressure to compact the laminate against the mold and create contact between each plies.

The consolidation and curing process was done by following the resin temperatures specification shown in Table 3.1. Thermoplastic prepregs are generally processsed at the melting temperature of the resin [9]. The process cycle time for thermoplastic composites is much faster than thermoset composites, in the range of a few minutes. The consolidation and curing pressure during cycle of the produce laminate is shown in Figure 3.5. The set point temperature is 377°C, of which according to its resin properties. Meanwhile, the starting pressure is 2 bar. When the temperature reaches 377°C, the pressure is increased to 8 Bar, and dwelled for 20 minutes. After dwelling time, the pressure is kept constant and temperature is reduced with 5°C/min. When it is below glass transition temperature, the pressure is reduced with 0.1 Bar/minute. The laminate is taken after the temperature is below 50°C.

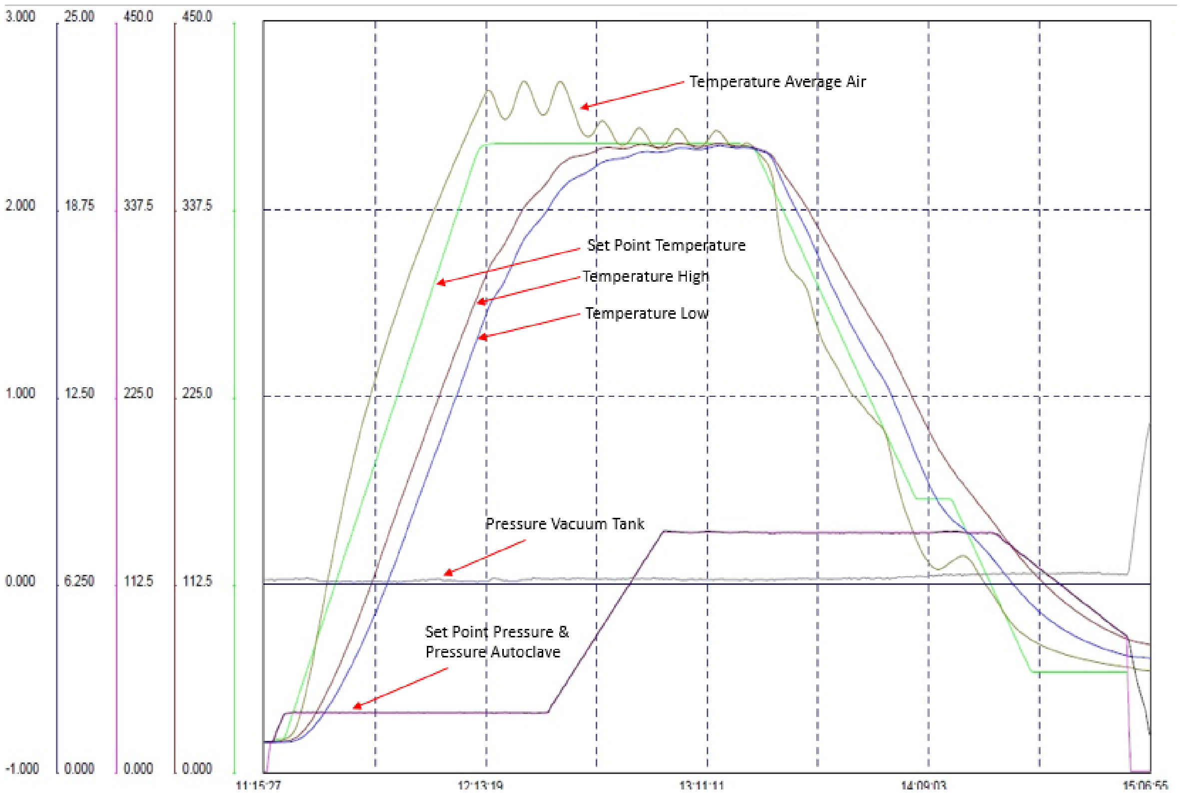

Figure 3.5: Consolidation and Curing Cycle

Table 3.1: Toray Cetex® TC1320resin properties

Property	Value
Density (specific gravity)	1.30 g/cm3 (80.5 lb/ft3)
Tg (glass transition)	160 \degree C (320 \degree F)
Tm (melt)	337 \degree C (639 \degree F)
Tc (crystallinity)	265 \degree C (509 \degree F)
Tp (processing)	370 - 400 \degree C (700 - 750 \degree F)

Figure 3.6 shows the C-Scan of the laminate. Although, it does not provide void contents information, it is possible to generalize that the laminates is relatively good. Three point bending test is conducted to measure the specimens stiffness. The idea is to perform a non destructive three-point bending. The specimen is only deflected at its mid length for 1.5 mm. The average flexural stiffness variations from different positions of the laminate are 12.79 N/mm with standard deviation 0.80.

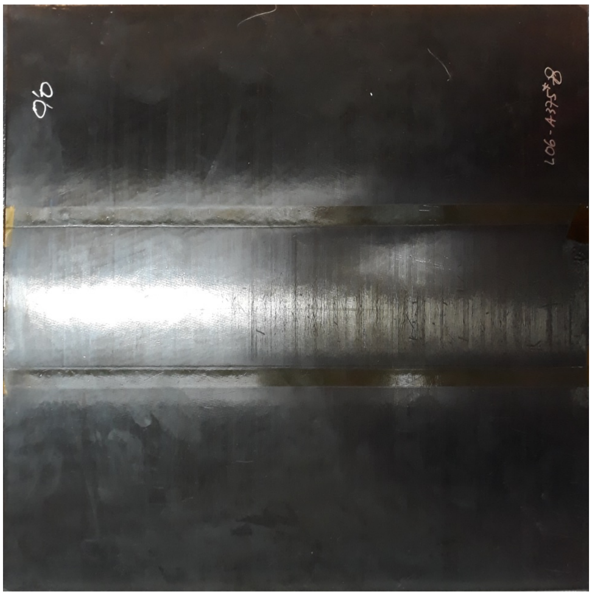

(a)

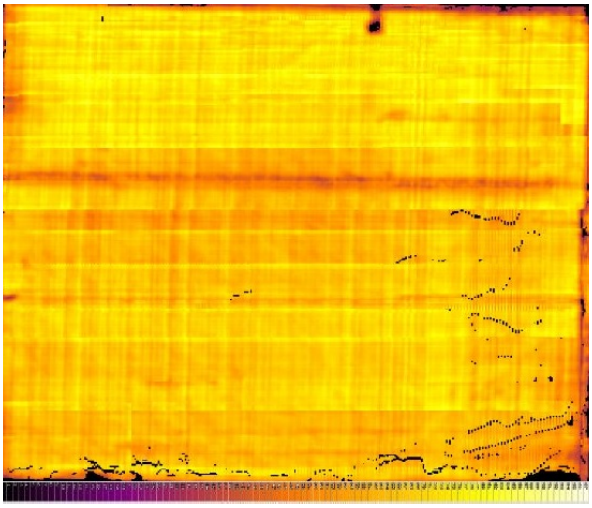

(b)

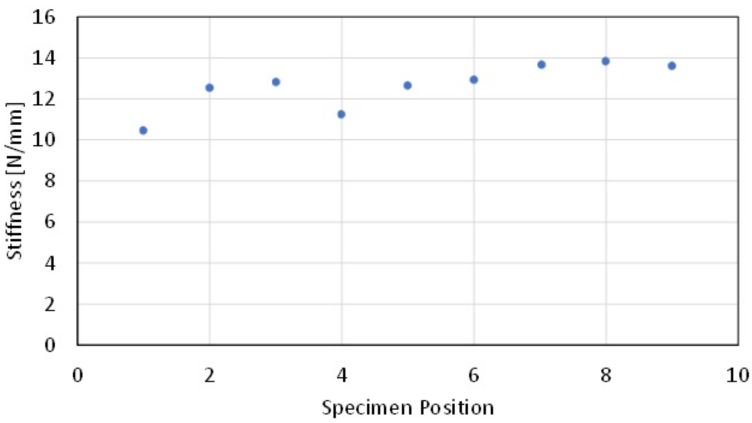

(c)

Figure 3.6: (a) UD laminate produced from Autoclave (b) C-Scan of the UD laminate (c) Stiffness variation from 9 different positions of laminate UD

Chapter 4

Vibration Fatigue Test

This chapter covers structural dynamics study on thermoplastic matrices using a high cycle fatigue on vibration loading testing. The results give an understanding on structural integrity change of ply-drops thermoplastic-based composite, which is reflected by stiffness degradation, response phase, amplitude base acceleration trace, and resonance frequency decay caused by the crack propagation. As it has been discovered during finding the correct specimen for the study, to accelerate the degradation of the specimens a pre-existence crack is made.

4.1 Description of Vibration Test Rig

Figure 4.1 shows the sketch of vibration fatigue testing rig. The idea of the rig is to provide the capability to test specimen, component or structure, by vibrating the specimen to its resonance frequency, and hence allowing the degradation of the specimen's structural integrity; In real time can capture the dynamic parameters of the specimen. It is equipped with electromagnetic shaker as a base acceleration to excite the specimen and a Polytec OFV 303 Sensor Head Laser Doppler Velocimetry (LDV) to capture the response velocity of the specimen. A reflection tape is attached to each specimen to boost the acquisition quality. The base acceleration is picked up by accelerometer.

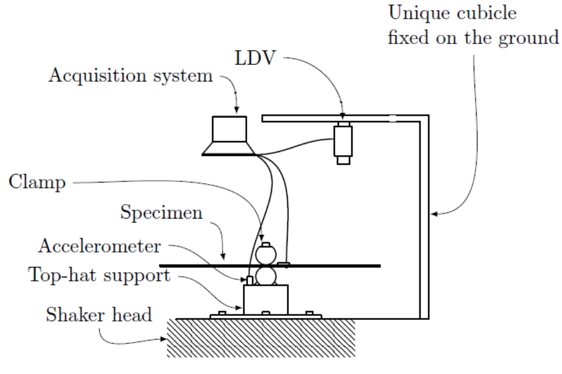

Figure 4.1: Vibration Fatigue Testing Rig [5]

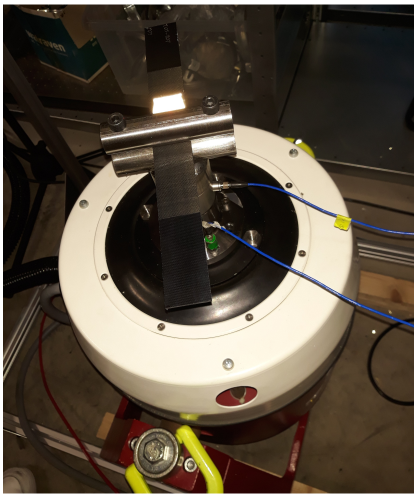

Figure 4.2: Fixture and its specimen

The software employed for data acquisition of the test is the MONTEVERDI software. MONTEVERDI is a software suite, coded in LabVIEW and is designed for carrying out automated vibration fatigue testing [16]. It is used to monitor, control and acquire data from the endurance tests. The MONTEVERDI software acquire the trends of phase shift, excitation frequency, amplitude, and acceleration.

Acquiring data through MONTEVERDI consists of several steps, which have to be performed sequentially. The first step computes the FRF of the velocity response signal coming from the Laser Doppler Vibrometer (LDV) pointed on the specimen, normalised by the input force. Due to the fixture used to connect the shaker to the component, it was not possible to normalise the output signal to the actual input force, as the latter could not be measured. The base acceleration was used instead; Strictly speaking the ratio in this case gives Transmissibility.

After measuring the FRF, the bandwidth of interest chosen; This bandwidth is around the resonance frequency. The bandwidth is normally around 1-2 Hz. Consequently, the software carries out a Stepped Sine Test (SST) using different excitation amplitudes. Incidentally, the SST is required to compute the FRF at high vibration amplitudes, close to the levels reached during fatigue testing, which are difficult to achieve with a pseudo-random excitation. Once the frequency sweep is completed and the broadband and stepped sine FRFs are saved, the fatigue test is proceeded.

MONTEVERDI employs two control systems during the endurance test, a Phase Lock Loop (PLL) control, and an amplitude control. In order to maintain the resonant conditions on the selected resonant mode, the PLL modifies the excitation frequency in order to match a given phase difference between the load and the response. However, the PLL is not used to allow the phase response shifting instead using its resonance frequency changing. Simultaneously, the amplitude control changes the input voltage to the shaker in such a way to keep the vibration amplitude constant, which will result in a constant strain level. When the endurance test is stopped, the final FRF is carried out again. The results is used to compare modal properties before and after fatigue.

4.2 Experimental method

In their work [5], [16], Magi & Maio proposed a new method to capture damage initiation and structural degradation during a fatigue test by exploiting resonance vibrations. The method employs monitoring dynamic parameters, including the phase angle between excitation and response, which changes as the overall stiffness changes as a consequence of damage. The approach to describe emerging scenarios is based on the equations of motion which is presented in Equation 2.14, and Equation 2.15. The analytical solution shows that any small stiffness variation is amplified by the dynamic response of the component as a large phase change, even when it is too small to be captured by the quasi-static response. Figure 4.3 shows the small change in stiffness is captured by the phase response.

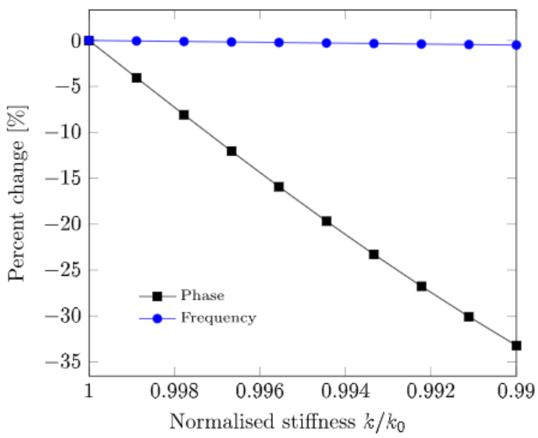

Figure 4.3: Comparison between change in resonant frequency and change in phase for a small change in stiffness of a SDOF system with 1% damping [7]

The experimental evidence of a critical event in the fatigue life of a component is found both in the dynamic phase shift and base acceleration magnitude trace. The critical event is captured from an abrupt change in the dynamic parameters of the structure as soon as a delamination is initiated. One case from a single fatigue test and by plotting the phase versus the logarithm of the number of cycles, one obtains the graph in Figure 4.4. The occurrence of critical event, the initial stage of microcracking before delamination, is confirmed with thermography in Figure 4.5.

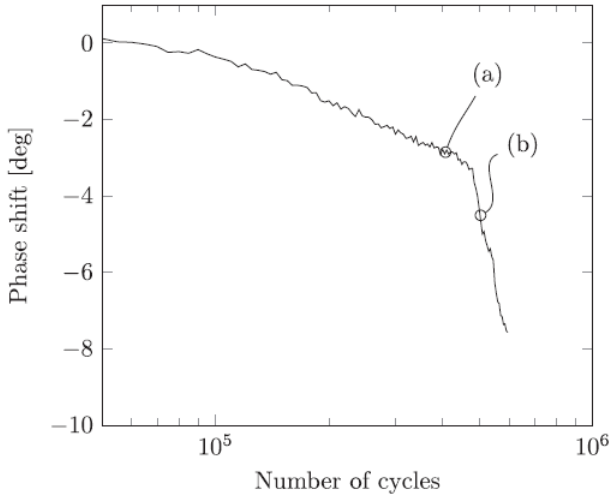

Figure 4.4: Typical bilinear behaviour/bilinear law in a logarithmic scale for the phase measurement during fatigue. (a) before critical event (b) after critical event [7]

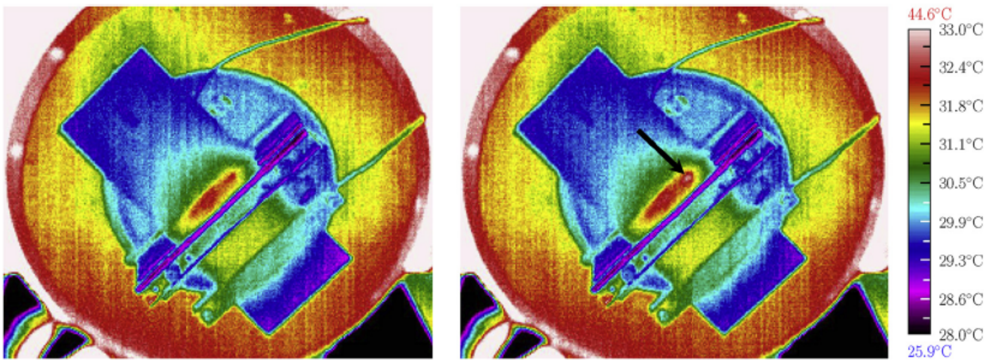

Figure 4.5: Thermal images of the top surface of the specimen from Figure 4.4 (a) before and (b) after the critical event. The delamination is indicated by the arrow [5]

Testing Condition and Procedure

All the fatigue tests are conducted in a storage room at room temperature (15°C). The temperature change is not affecting the strength of the specimen, since thermoplastics have elevated service temperature. This particular material has glass transition temperature of 160°C [31].

During the first trials, the stiffness of each specimen was measured by means of a three-point bending test using a ZwickRoell. Since the purpose is to measure the relative stiffness change before, and after the test, later on, it is found that the relative stiffness reduction can also be representative through calculation of modal stiffness. It is also to avoid the unexpected extension of crack during three-point bending test.

The high cycle fatigue test to determine the aimed amplitude for crack propagation was first performed. Since the software is performing high cycle fatigue test with constant amplitude, the amplitude to give the threshold is firstly fine tuned. Figure 4.6 shows the results of the specimen for different amplitude. The fixed amplitude is held during the propagation of the crack until a defined stopping criterion is reached. This stop criterion is established in this work by first determining when the expected crack is reaches up to 8 mm without test intervention. Intervention is needed in this case when the actual resonance frequency has move away from the set excitation frequency, hence, the excitation frequency is adjusted to keep up the constant amplitude, which has been further explained in the previous Section 4.1.

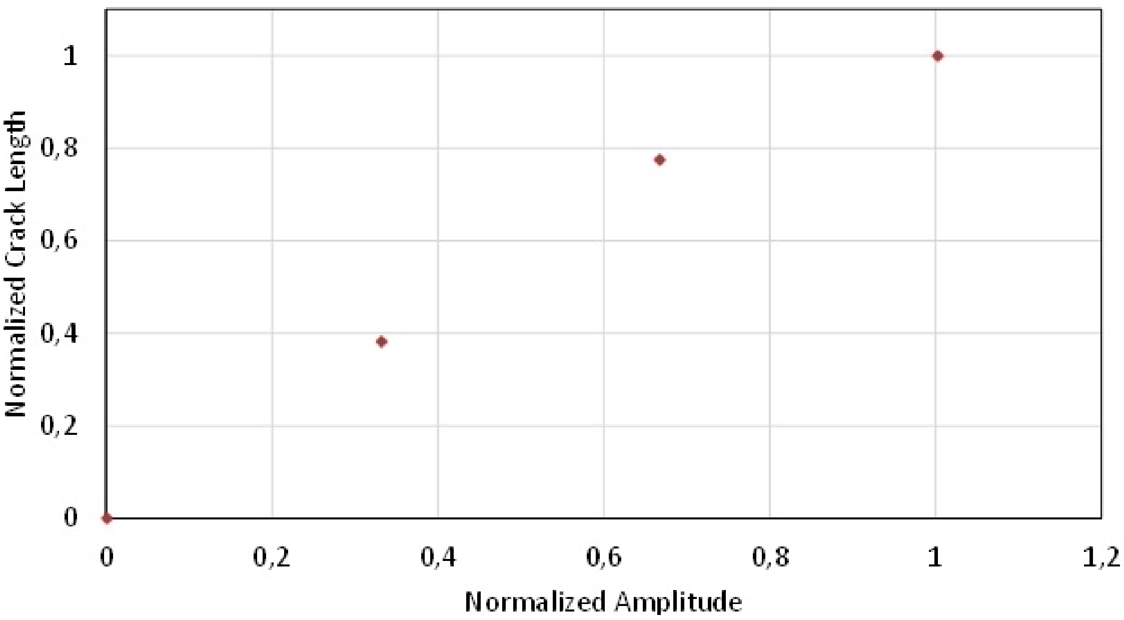

Figure 4.6: Normalized amplitude against normalized crack

The aimed amplitude determines the severity (strain/stress) of the specimen during the vibration testing. The measurement point of aimed amplitude is critical in ensuring the same severity throughout different tests. On the longitudinal direction, it will change the severity. Moving the laser along the width direction is giving the same severity. The higher the aimed amplitude is, the faster the crack propagate, thereby the faster the occurrence of stiffness degradation.

When the amplitude is constant, the opening of crack is dependent on the number of cycles. The test up to 8 mm without intervention is established as the longest number of cycles test. Afterwards, multiple tests with different number of cycles are conducted with different specimens in between the longest cycle, to get the fine resolution for propagation rate.

All tests are carried out with FRF test before, and after the High Cycle Fatigue (HCF). This procedure are applied to all specimens of UD, and 0-90. After preparing the specimen, the first step in MONTEVERDI is determining the Frequency Response Function (FRF). Figure 4.7 is a visual representation of the resonance frequency results of one specimen before and after vibration testing from FRF. for these type of specimens, the resonance frequencies were found to be in the range of 206 Hz which is found to be still fit within the operational capability of the electromagnetic shaker.

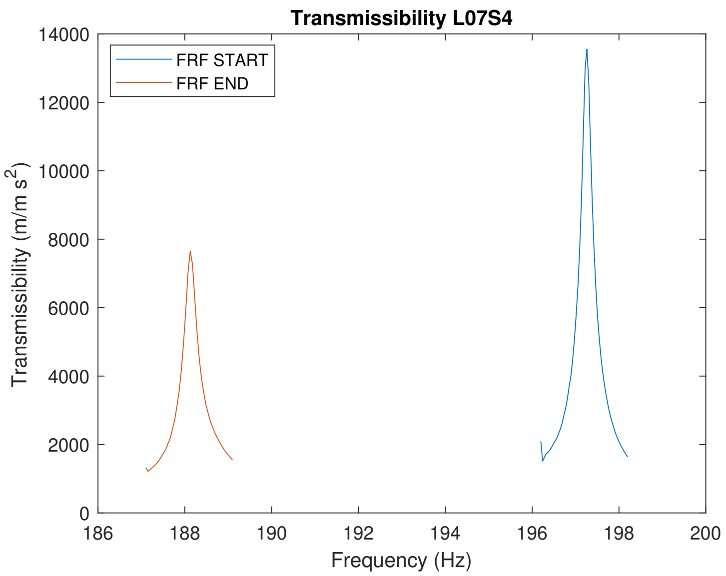

Figure 4.7: One of the FRF test, FRF specimen L07S4

The centre lines of the specimen are mounted onto the clamp of the shaker. Hence, the specimen is mounted symmetrically. The accuracy is ensured each time the specimen is mounted by measuring the distance and ensuring the specimen is perpendicular to the clamp edge. The ply-drops edge is 35 mm from the contact point of clamping force such that the crack growth will not experience the compression force from the clamp, which can influence the results. Both ply-drops edges have an equal distance to clamping line of contact. It is to ensure that the crack will propagate naturally without constraint from the clamp. Crack length of maximum 8 mm is expected from the test. In order to ensure there is no excessive tighten and mismatch, which can cause different constraints, the clamps is always sequentially tighten with mechanical preset torque up to 7 Nm. Higher torques can crush the fibre/resin under the clamp [16].

4.3 Effect of Vibration Test and Failure Identification

Initially, the definition of the criteria and methods used for studying vibration fatigue behaviour for this specimens is established. The failure criteria of the specimen can be finally determined after gaining experience in testing different type of specimens during this work.

Additionally, characterization of the failure events is of importance before gaining the understanding of which specimen will give the right severity for structural degradation, as well as, the structural performance of the ply-drop composite. It was done by characterizing the failure event, while at the same time monitoring the dynamic parameters behavior, more spesifically phase degradation within the failure events. The crack is monitored each time the test was finished by a digital microscope. The method that has been explained in the Section 4.2 employed to understand both specimens behavior.

Failure event is associated with a sudden change of phase shift caused by the cracks opening. According to Magi [7], [16], It is possible to divide the component life in three phases which has been explained briefly in the Section 2.2. Nevertheless, this work established a set of events which is capturing the real case with ply-drops component with pre-crack feature. The first event is event where the excitation frequency is adjusted to keep the phase around its resonance. Hence, the occurrence of this event ranging up to 70.000 cycles depending the smoothness of excitation frequency adjustment to keep it around its resonance phase. Noteworthy to mention, this adjustment is only on this first phase. Afterwards, for both specimens the occurrence of the first and second event are allowed without changing the excitation frequency. Hence, there is no significant fluctuation of amplitude, phase, and base acceleration. It then guarantee that the stress applied to the specimen, is not changing over the course of the test. This is of importance to be able to study the crack propagation. The measurement is started on the second and third event.

1. The first event is a period when the opening of polymide (seeded crack). The phase shift is degrading fastly. The micrograph shortly after this event is shown in Figure 4.8. This event occurs from the beginning of the fatigue test up to 70.000 cycles.

2. After the first event, the phase shift is constant. The second event is the phase up to where the crack is visible (measurable), of which arround 0.10-0.20 mm. The measurable crack is defined by the ability of the digital microscope to capture the image.

3. The third event is when the crack is started to propagate along the matrix. The second event is when the stiffness changing occur on the specimen. When looking at the phase shift decay, it is when there is a sudden change on the phase shift after the second event. This third event is further studied from Section 4.3.1.

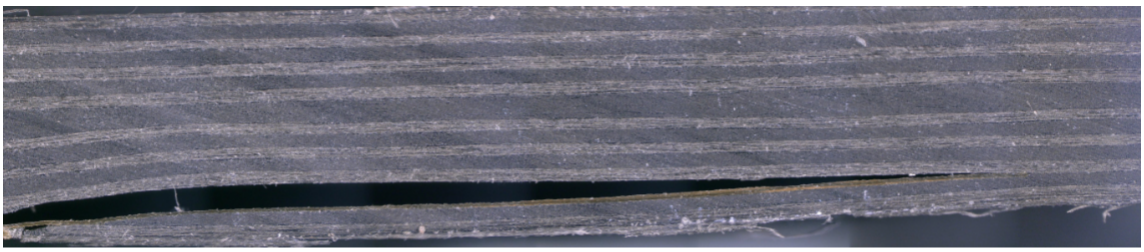

Figure 4.8: Opening of the polymide during the first event

4.3.1 Crack Growth Rate Ply-Drops

By following the understood critical event, the UD specimen UD is allowed to fail until its third event. The results can be seen in Table 4.1. Specimen UD is showing scatter data across all 4 spots. it is found due to fibre bridging [8]. In the DCB test, fiber bridging also has been found to increase resistance to delamination. However, when the maximum length is plotted, as the cycle increase the initiated crack is propagating. The results of maximum crack length over the number of cycles can be seen in Figure 4.9.

Table 4.1: Crack Growth Specimen UD

Specimen	A (mm)	Cycle [10^6]	Crack Growth (mm)			
			Spot 1	Spot 2	Spot 3	Spot 4
L06S2_250	0.85	0.25	0,87	0,54	0,42	0,60
L07S5	0.85	0.3	0,00	0,13	0,00	0,28
L07S5_300	0.85	0.4	0,00	0,00	0,00	1,65
L06S3_400	0.85	0.53	1,67	0,00	0,13	0,01
L06S3	0.85	0.55	5,54	3,35	1,00	5,18
L06S5	0.85	0.64	4,79	0,14	0,00	0,00
L06S2	0.85	0.64	5,74	1,17	1,23	5,84
L07S4	0.85	0.64	8,84	0,00	0,00	0,00
L07S7	0.85	1.2	19,39	4,82	15,98	5,92

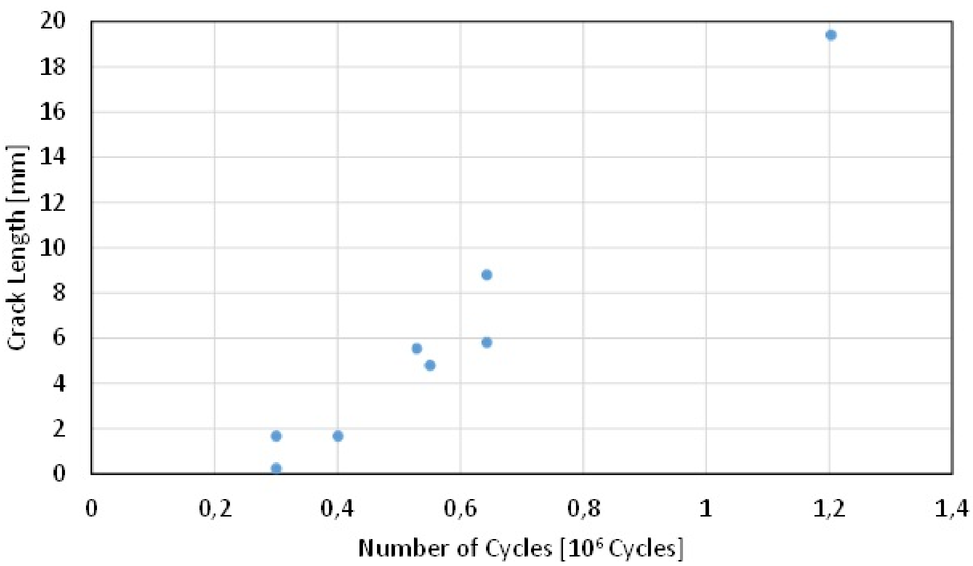

Figure 4.9: Crack length over a number of cycles on specimen UD

Cracks in specimen 0-90 are found to exhibit uniform growth. A very minor deviation found due to the crack travel to fibres area which give different propagation rate. One of the cases that shows the result of a very small deviation at the longest cycles can be seen in Figure

4.10. The cracks in spot 3 and spot 4 are found to travel to the fibre area, which reduces the crack propagation slower compare with the two other spots. It is also the same case with the spot 1, which reached the fibre area faster then spot 2. It consequently gives a lower crack length in spot 2. Nevertheless, considering spot 1, and spot 2 are from two opposites side of cantilever, it gives reasonable equal length of delamination on each side of cantilever. The results can be seen in the Figure 4.9.

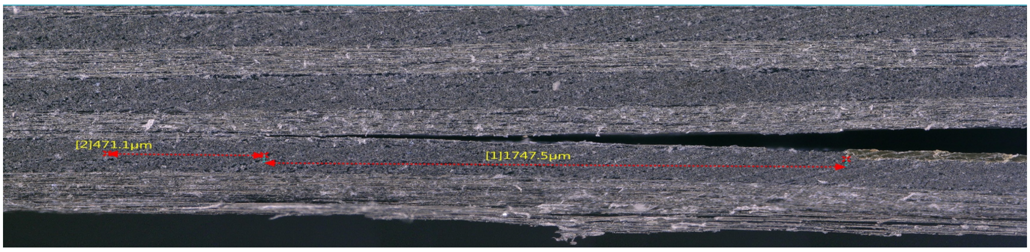

(a)

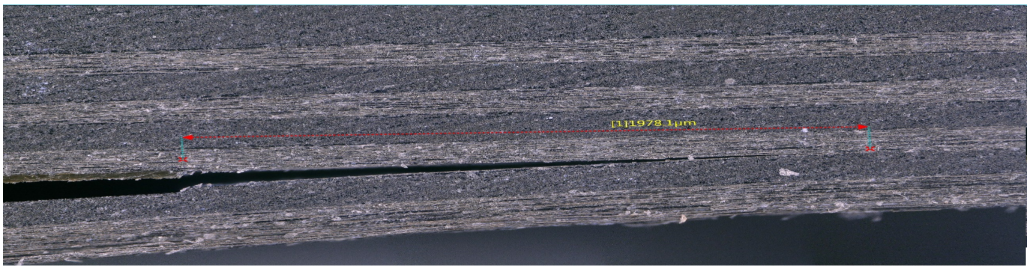

(b)

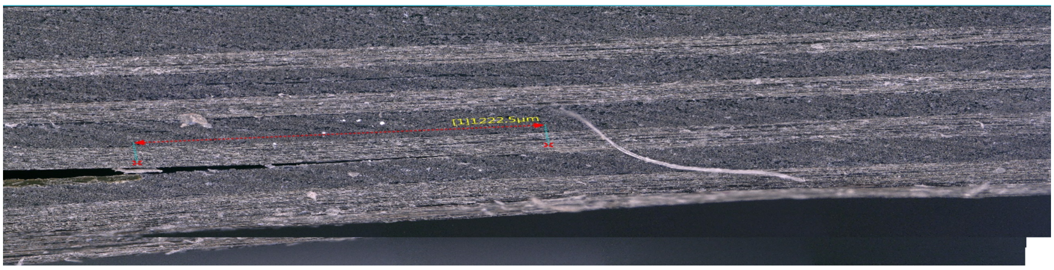

(c)

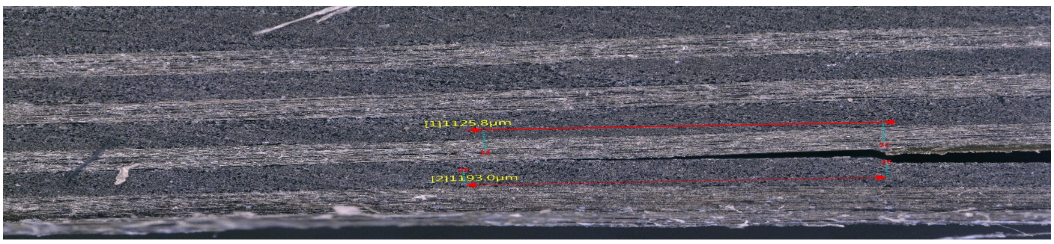

(d)

Figure 4.10: Micrograph of L08S3 run at 1.2 amplitude for 1.5 million cycles (a) Spot 1 - 1.75 mm crack (b) Spot 2 - 1.98 mm crack (c) Spot 3 - 1.22 mm (d) Spot 1.12 mm

Furthermore, it is found that a higher strain is required to open the crack for specimen 0-90 to initiate crack relative to the UD specimen. Specimen 0-90 requires 1.2 amplitude in order to initiate and propagate crack, meanwhile, 0.85 for specimen UD has already given more severe crack with less cycles. As mentione earlier. in specimen 0-90, it is also found that the crack open uniformly starting from the edge of ply-drops along the length of ply-drops. The results of crack size over its number of cycles are shown in Figure 4.11.

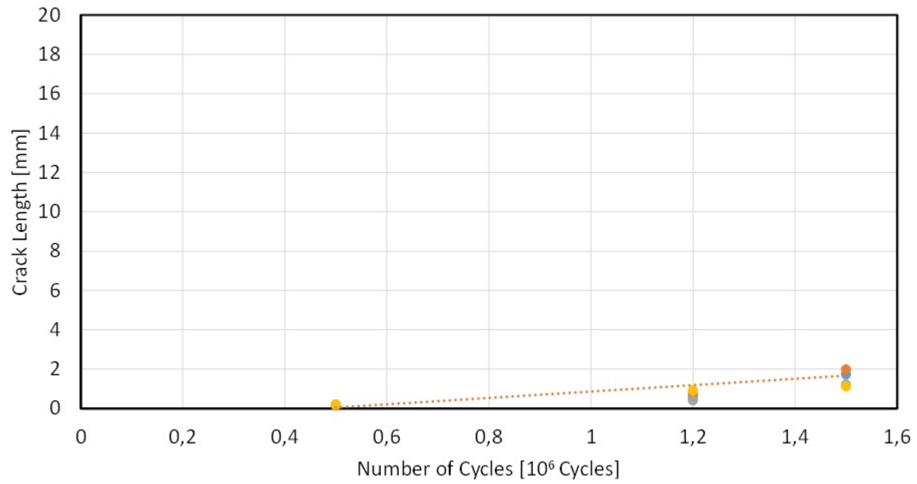

Figure 4.11: Crack length over a number of cycles on specimen 0-90

From Figure 4.12, it clearly presents that propagation rate of specimen UD is higher than specimen 0-90; It is one order of magnitude higher. The propagation rate in this case is average since it comprises of different cycles and specimens. The average propagation rate of specimen UD is 2E-5, meanwhile, the magnitude of specimen 0-90 is 2E-6. R squared 0.9669 and 0.9008 for specimen UD, and 0-90 respectively.

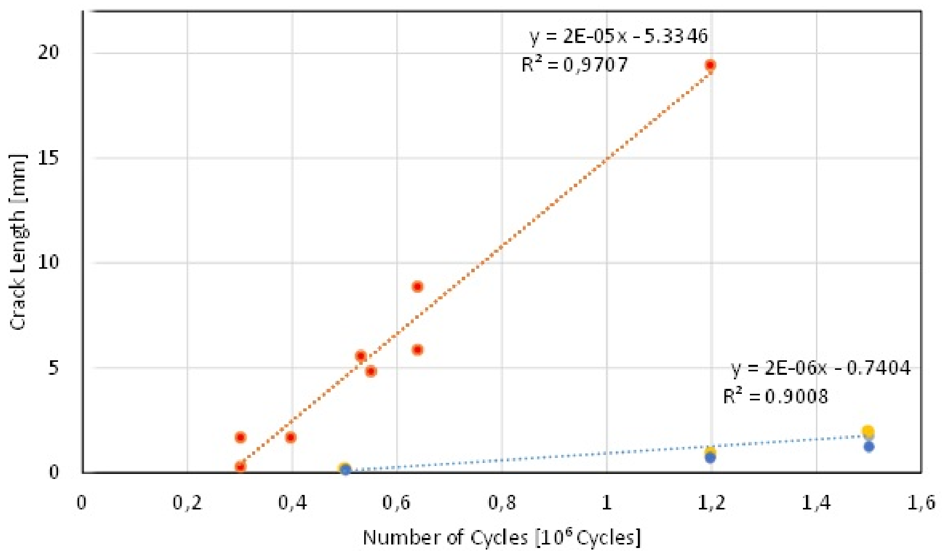

Figure 4.12: Propagation Rate Specimen UD and Specimen 0-90

4.3.2 Dynamics Parameters Effect

Specimen UD

The rate of change of the response phase shift presents a slope, which describes the explained critical event, as well as, the crack growth propagation rate on the specimen. The period of cycles where the first event, the opening of the seeded crack, occur is omitted. Hence, the graph is shown when the cycle starting from 70.000 cycles. As has been explained briefly, the occurrence of the third event —the crack propagation —, is captured until the base acceleration reaching 9 Volt in order not to intervene the test. The response phase shift for specimen UD is shown in Figure 4.13.

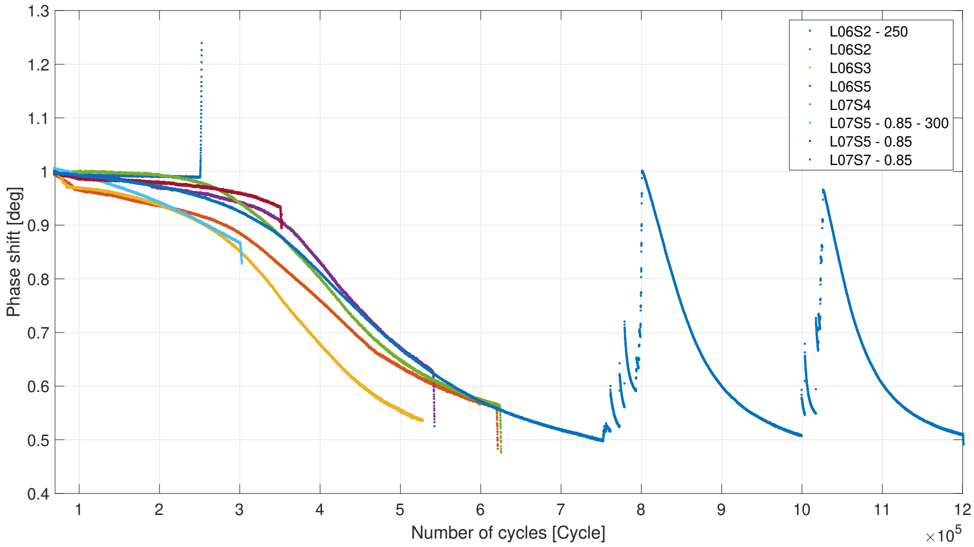

Figure 4.13: Phase Response Shift Specimen UD

The results of the modal stiffness reduction, phase shift decay, resonance frequency decay, and increased damping of specimen UD are shown in Table 4.2. It is obvious that the crack from fatigue test has a changed stiffness distribution caused by crack opening. The resonance frequency in Table 4.2 is,—as well as other parameters —,measured before, and after the test.

Table 4.2: Dynamic Parameters Changing of specimen UD

Specimen	Cycle [10^6]	Reduction (%)			Increase Damping (%)	Max length (mm)	Total Crack (mm)
		Stiffness Reduction	Resonance Reduction	Phase Shift Reduction			
L06S2_250	0.25	n/a	0.04	0.16	22.92	0.87	2.42
L07S5	0.3	0.76	2.88	14.00	334.72	0.28	0.41
L07S5_300	0.3	0.76	0.00	0.00	78.48	1.65	1.65
L06S3_400	0.4	0.01	0.01	4.34	0.42	1.67	1.81
L06S3	0.53	3.25	4.33	48.03	116.00	5.54	15.07
L06S5	0.55	2.61	1.83	38.79	39.86	4.79	4.93
L06S2	0.64	3.45	4.20	48.31	116.13	5.84	13.98
L07S4	0.64	3.70	4.63	45.20	149.38	8.84	8.84
L07S7	1.2	13.52	8.59	0.00	189.61	19.39	46.12

The Phase shift of specimen UD can be used to capture the total crack length regardless of which spots are delaminated. However, the characteristics relation between crack-resonance-stiffness in specimen UD is not as entirely clear as specimen 0-90, which will be shown in next section. The plotted data can be seen in Appendix B.

Specimen 0-90

The rate of change of the response phase shift presents a slope, which describes the change of the critical event, as well as, the crack growth propagation rate on the specimen. The period of cycles where the first event, the opening of the seeded crack, occur is ommited. Hence, the graph is shown the cycle starting from 70.000 cycles. The response phase shift for specimen 0-90 is shown in Figure 4.14.

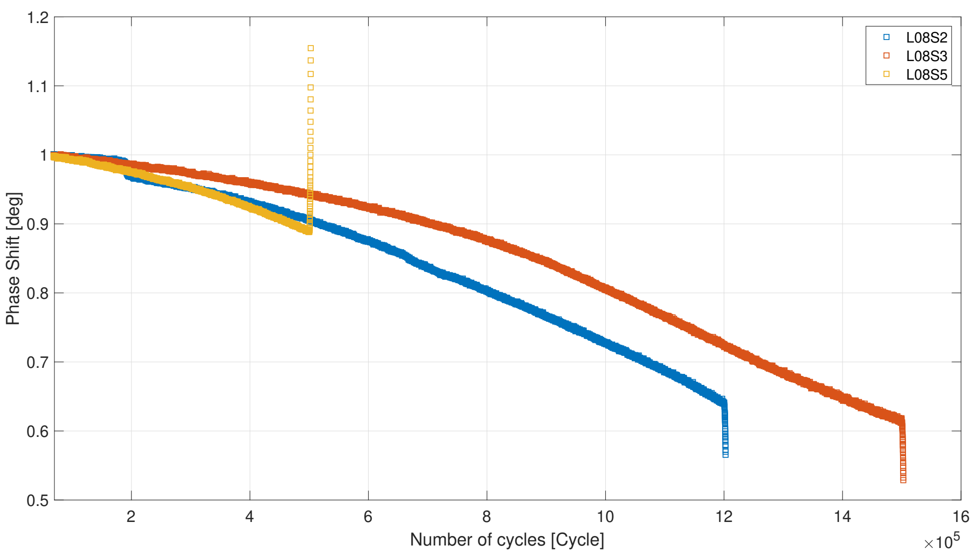

Figure 4.14: Phase response shift specimen 0-90

In the case of specimen 0-90, because of the uniform delamination the phase shift can accurately be used as a measurement of the cracks. Meanwhile, specimen UD was stated possible but not accurate. The results of dynamic parameters change on 0-90 is shown in Table 4.3.

Table 4.3: Dynamic Parameters Changing of specimen 0-90

Specimen	Cycle [10^6]	Reduction			Increase	Total
		Stiffness	Resonance (%)	Phase Shift (%)	Damping (%)	Crack
L08S5	0.5	0.45	3.33	11.35	41.38	0.67
L08S2	1.2	0.78	3.63	35.8	56.28	2.67
L08S3	1.5	0.99	3.87	38.66	62.95	6.07

In Figure 4.15, the crack is related to resonance frequency decay, and stiffness reduction. The resonance frequency decay slope is found the same with the stiffness reduction's, 1.79, and 1.80, respectively. It is, obvious since, resonance frequency is proportional to square root of stiffness as in Equation 2.10. It is, as well as, because of the uniform crack growth developed during the course of delamination growth. Hence, it can be concluded that resonance frequency is able to accurately capture the stiffness degradation of the specimen 0-90, which simultaneously able to capture the crack length. Resonance frequency degradation can be a good indicator of how long crack has developed. When the resonance frequency and stiffness is tracked over the number of cycles, as shown in Figure 4.16, it is showing good agreement with the finding.

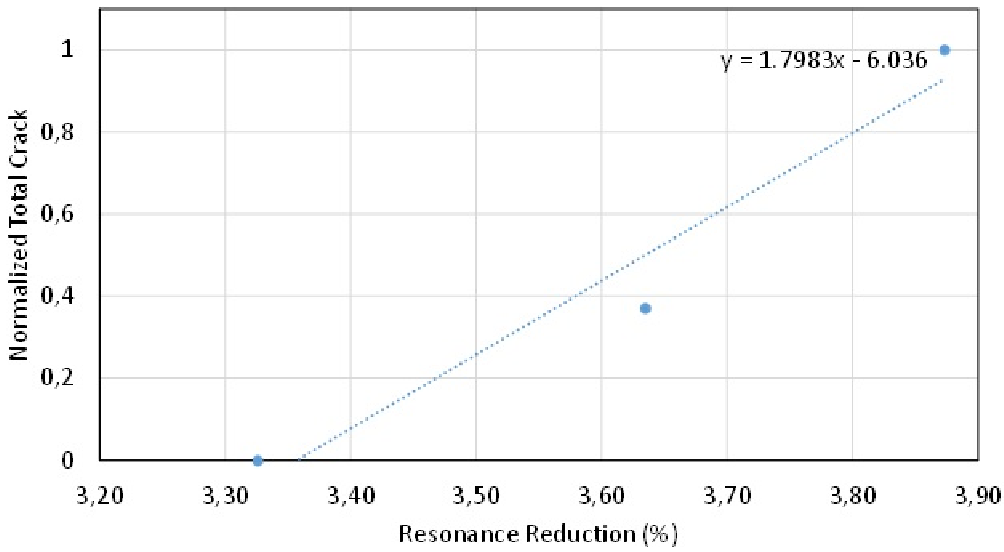

(a)

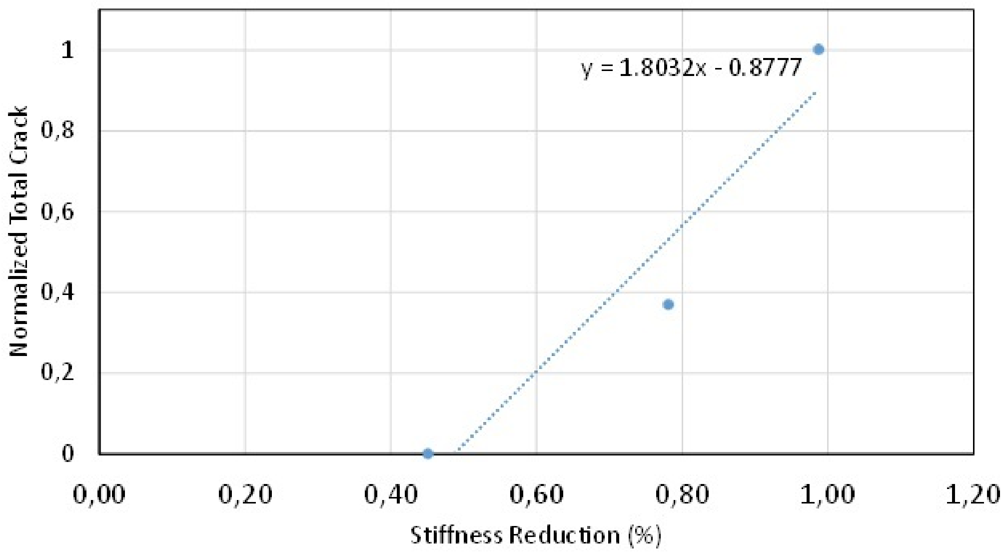

(b)

Figure 4.15: Crack vs (a) Resonance frequency reduction and (b) stiffness reduction Specimen 0-90

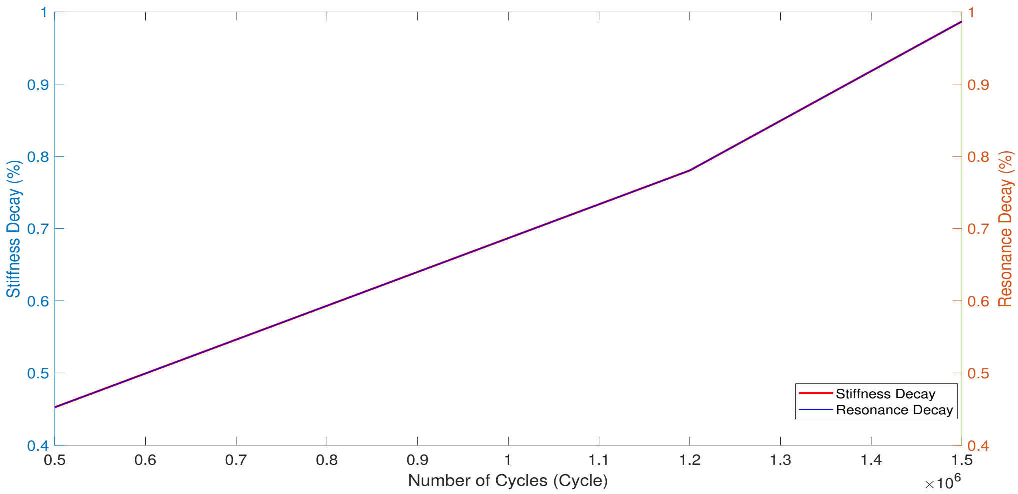

Figure 4.16: Stiffness decay and resonance frequency decay specimen 0-90

As has been found earlier in Section 4.3.1, specimen 0-90 requires higher amplitude to initiate cracks, it also takes considerably longer cycle to develop crack compare to specimen UD. The comparison is shown in the Figure 4.17 through phase response shift. This exhibited behaviour will be further studied and explained in Chapter 5. The response phase shift for both specimens are shown in Figure 4.17 for different number of cycles.

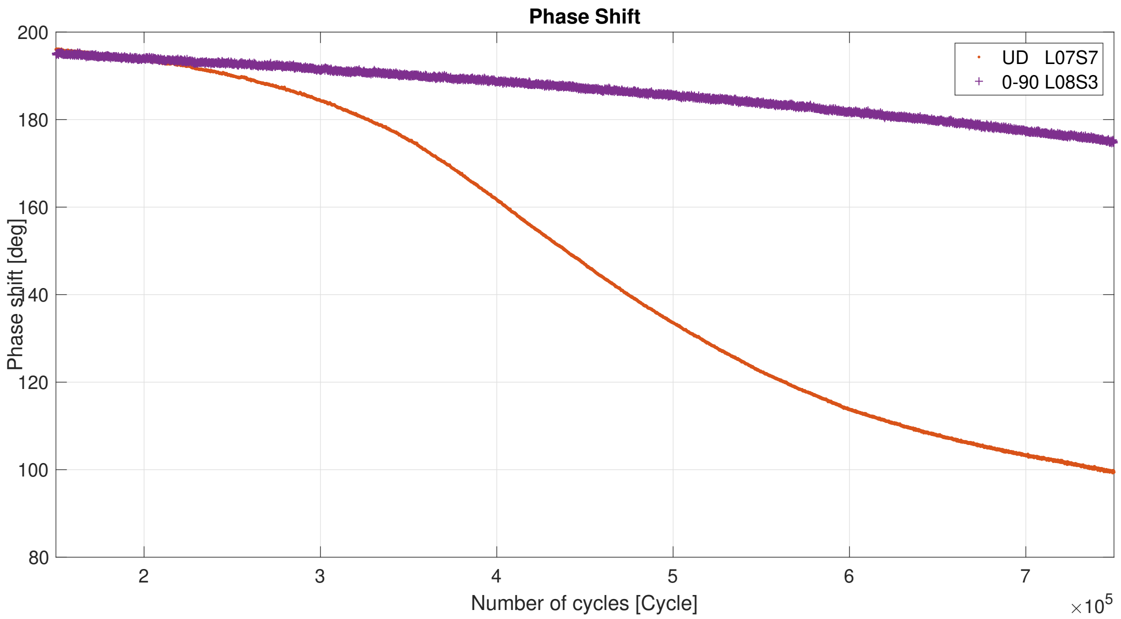

Figure 4.17: Phase Shift Decay of specimen UD and specimen 0-90

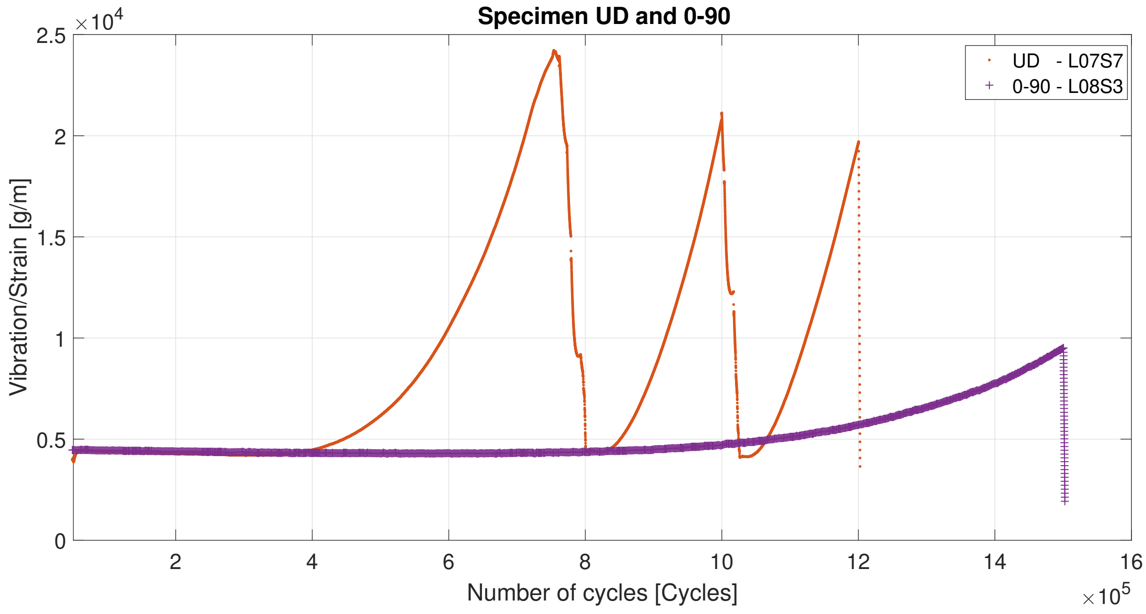

Figure 4.18: Base Acceleration Trace Normalized of specimen UD and specimen $0-90$

Phase Shift and Base Acceleration

The trace of base acceleration magnitude can also be a guidance to check the propagation of measurable crack. However, it is less sensitive in capturing the transition from the second event to the third event where the origin of propagation starts to take place. It is because the changing of stiffness is still very limited during this period. It is also explainable with the Equation 2.12. The change of specimen stiffness cause the change of base acceleration in order to keep the displacement constant. Meanwhile, during the initiation of a crack, the change of stiffness is considerably lower. As has been explained earlier, in this experiment, the displacement, which translates as amplitude is kept constant. The origin of the third event that has occured from 250.000 cycles for UD can be seen clearly in Figure 4.17, meanwhile it is still not capturing the stiffness degradation in acceleration trace. Through base acceleration trace in Figure 4.18, it is only obvious after 400.000 cycles.

.

Chapter 5

Crack Growth Law Derivation

In this chapter, further characterization of fatigue of both specimens are determined. The strain energy release rate that influences the delamination growth is found through 3D FE model. Furthermore, delamination growth per fatigue cycle, da/dN from experimental result, is related to strain energy release rate, G from simulated model. At last, the ultimate aim of derivation crack growth law, which is an expression that relate delamination growth per cycle with strain energy release rate, G, is determined. The exponents of the power law relationship can be used as a crack growth prediction tool in the case of vibration fatigue loading.

5.1 Modelling Method

The Finite Element (FE) analysis is carried out in a 3D model with the use of ANSYS-software. This model is used to simulate the real experiment to understand the involving stress which is used to determine strain energy release rate (SERR). The model is employing an orthotropic solid body with its available physical and mechanical properties, hence, high-fidelity modelling on laminate is not the aim. Physical and mechanical properties for both specimens are shown in Table 5.1.

In order to address this purpose, a steady-state dynamic analysis (harmonic analysis) is performed. Prior to conducting harmonic analysis, the model is validated with a modal analysis. The same geometry with the same boundary condition as in real case is first modelled. It is found that the mode shapes of the model are identical to the mode shapes in experiment in UD Ply-drop. For specimen 0-90, the given properties are refined to get the same bending mode. These refined values are presented in Table 5.1 After the stress is extracted from the element, it is then used to calculate the strain energy release rate (SERR). The step by step procedure of the modelling is described in Figure 5.1.

Table 5.1: Material orthotropic properties of specimen UD and Specimen 0-90

Material Property	Specimen UD	Specimen 0-90
Young's Modulus X direction	135 GPa	72.5 GPa
Young's Modulus Y direction	124 GPa	72.5 GPa
Young's Modulus Z direction	124 GPa	124 GPa
Density	1590 Kg/m^3	1590 Kg/m^3
Shear Modulus XY	96.5MPa	96.5MPa
Shear Modulus YZ	5.2 GPa	5.2 GPa
Shear Modulus XZ	5.2 GPa	5.2 GPa

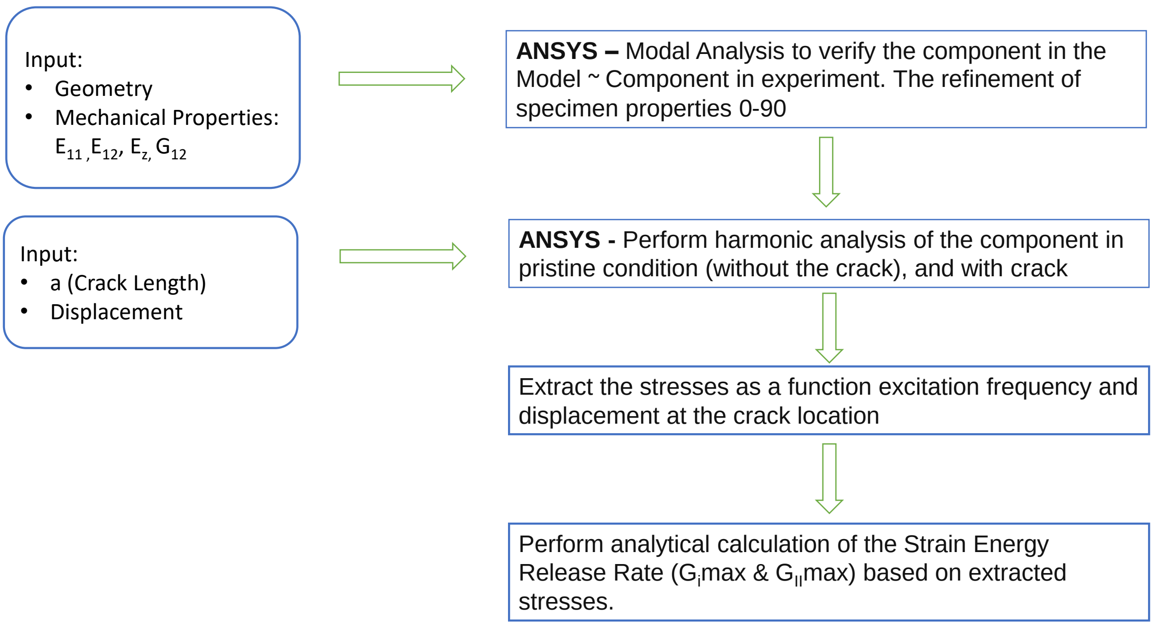

Once the SERR is found, it is plotted to da/dN, which gives the relationship between delamination growth rate and strain energy release rate (SERR). A power law relationship is found, which can be used as a crack growth prediction tool. Furthermore, for the case of 0-90 specimen, it gives uniform crack growth. Hence, the model is also further investigated with the case of crack occurrence. The crack occurred in the experiment is simulated in the model. Further details of each step is explained in the subsequent section.

5.1.1 Modal Analysis

The dimensions are exactly as described in section 3.2 except that it is with cantilever beam; Half symmetry of the specimen, considering that it is symmetrical with other side of cantilever of which giving the same modes. 5% difference of resonance frequency magnitude when simulated with full beam. The length of the cantilever is 126.5 mm and width is 27.6 mm. The boundary condition on the clamped side is fixed with 0 displacement on X,Y, and Z directions as can be seen in Figure 5.1. The model contains 20.646 elements SOLID186 with 14245 nodes. The element type is SOLID186 with quadratic element (HEX20).

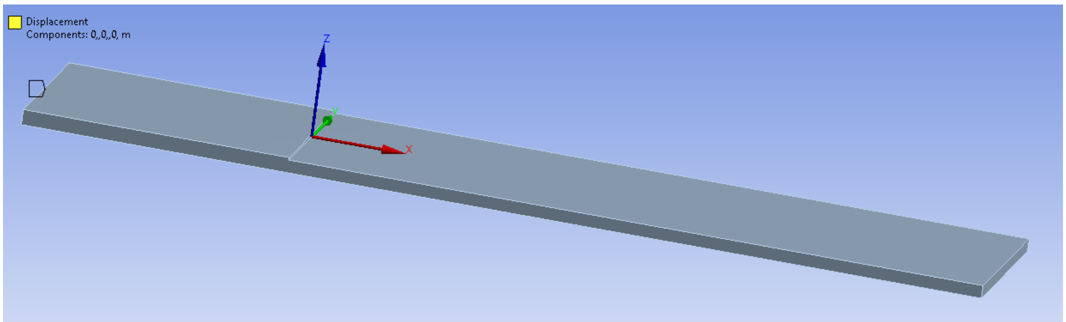

Figure 5.1: Cantilever ply-drop with boundary condition

In this section, the results of finite element (FE) 3D structural modal analysis of the ply-drop specimens are presented. The natural frequencies, and modes are extracted, analyzed and compare if they give the same characteristics (natural frequency and mode shape) as in the experiment. Convergence to validate the results are conducted, and shown in Appendix C. This ensure that the mesh is fine enough to capture the dynamic response in harmonic analysis in Section 5.1.2. Additionally, early on the experiment, modal analysis is also necessary to determine the excitation frequency range of the fatigue test. Sample of natural frequency at its 2nd bending mode from experiment can be seen in Table 5.2.

Table 5.2: Natural frequency of specimen UD and 0-90 at its 2nd mode from experiment

No	Specimen UD		Specimen 0-90	
1	Specimen	Natural Frequency (Hz)	Specimen	Natural Frequency (Hz)
2	L07S5	201.60	L08S5	164.79
3	L06S2	205.68	L08S2	160.18
4	L06S3	206.86	L08S3	160.10
5	L06S4	204.02	L08S8	161.68
6	L06S8	205.17	L08S9	162.56

The obtained values of natural frequencies of both specimens from model are presented in the Table 5.3. The results from modal analysis in the model is the same as from experiment. Noteworthy to mention, both specimens are run on its 2nd bending mode. Henceforth, model is confidently hold valid.

Table 5.3: Natural frequencies of specimen UD and 0-90 from model

Mode	Natural Frequency Specimen UD	Natural Frequency Specimen 0-90
1	186.24	137.30
2	204.59	160.38
3	483.73	473.74

The first three mode shapes are presented in Figure 5.2 and Figure 5.3, for specimen UD and 0-90 respectively. The mode shape of 2^{nd} mode of specimen UD is as shown in Figure 5.2 (b), and 2^{nd} mode shape of specimen 0-90 is in Figure 5.3 (b).

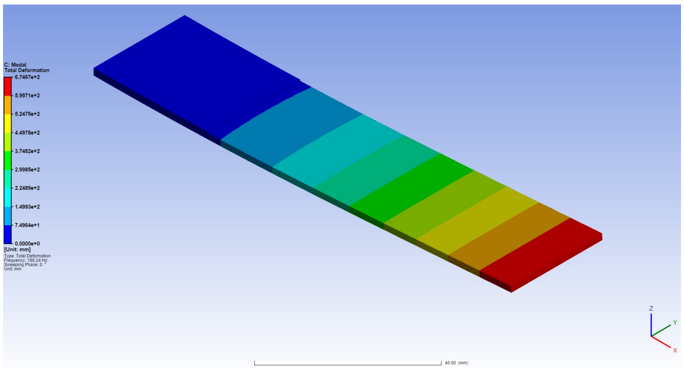

(a)

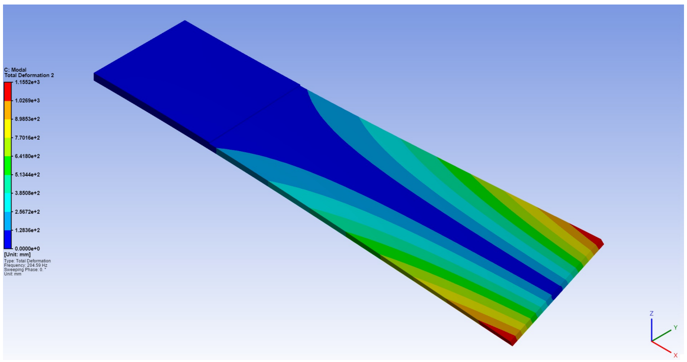

(b)

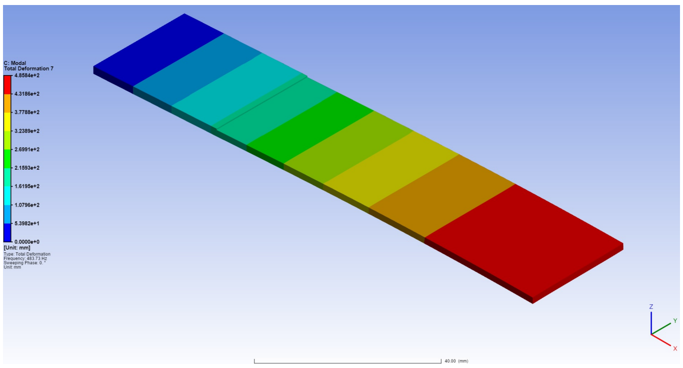

(c)

Figure 5.2: First three mode shapes of the specimen UD (a) Mode-1 1st bending (b) Mode-2 1st torsional (c) Mode 3- 2nd bending

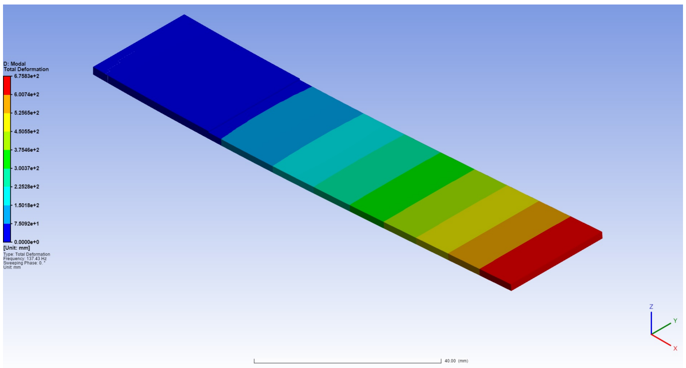

(a)

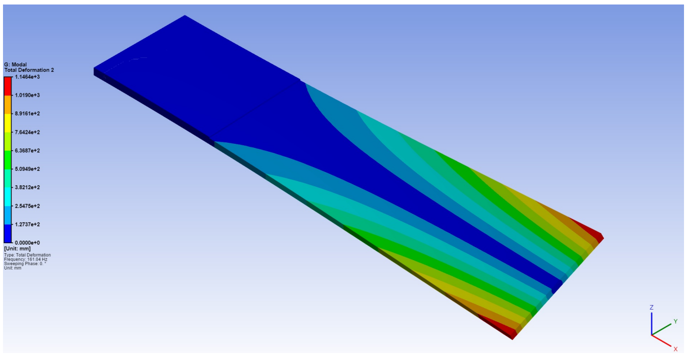

(b)

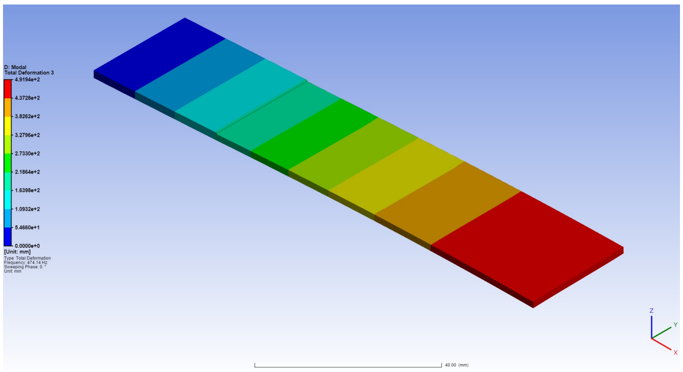

(c)

Figure 5.3: First three mode shapes of the specimen 0-90 (a) Mode-1 1st bending (b) Mode-2 1st torsional (c) Mode 3- 2nd bending

5.1.2 Simulation

The natural frequencies and mode shapes are used as starting point and validation for harmonic analysis. The polymide, which is used as a crack intiator gives instant reduction of natural frequency of 5 Hz (+/- 0.5 Hz) on the first 20.000-50.0000 cycles. Hence, as explained in Section 4.3.1, the excitation frequency is adjusted during the experiment to follow the natural frequency, which is also applied in this simulation. This value is employed as set excitation frequency for imposing steady-state dynamic analysis. The boundary conditions are assumed as follows.

1. The clamped side is fixed with 0 displacement on X,Y, and Z directions
2. The structure undergoes 0.85 from the edge of the clamp and 1.2 mm displacement on the Z direction for specimen UD, and B, respectively.

The 3D FE construction model that has been developed and verified with modal analysis is imposed with these boundary conditions. The model is using finite elements SOLID186, of which contains 20646 elements, 77646 nodes with shape of quadratic element (HEX20) for specimen UD, and 0-90. Distribution of stress of both specimens in pristine condition are presented in Figure 5.4, and Figure 5.5. This extracted stress is then used to calculate the related strain energy release using Equation 2.3, and Equation 2.4. The extracted stress are presented in Table 5.4.

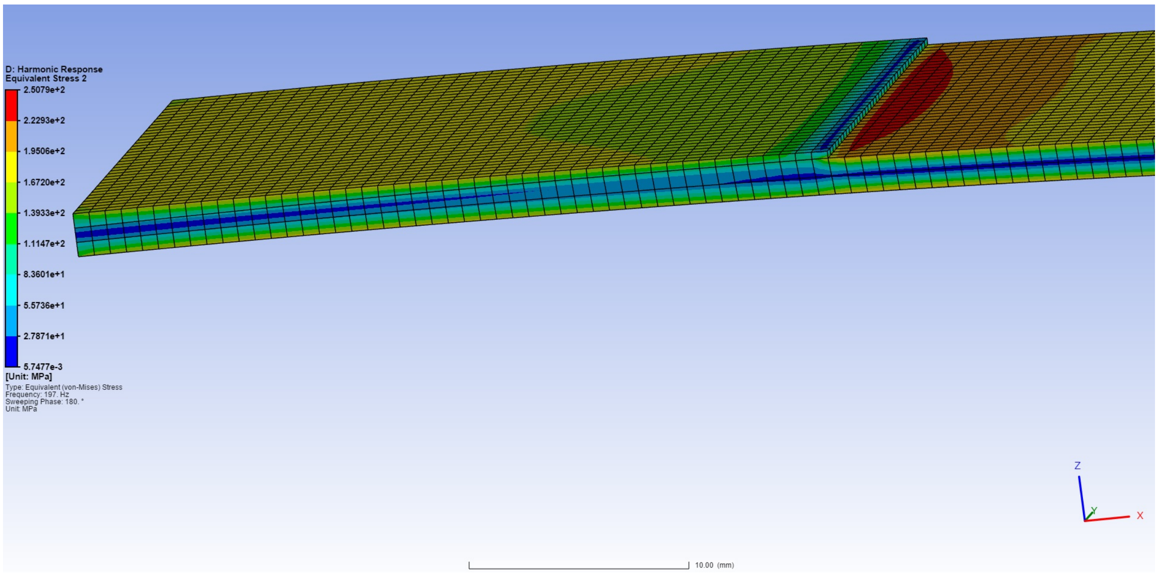

Figure 5.4: Stress Distribution on Specimen UD

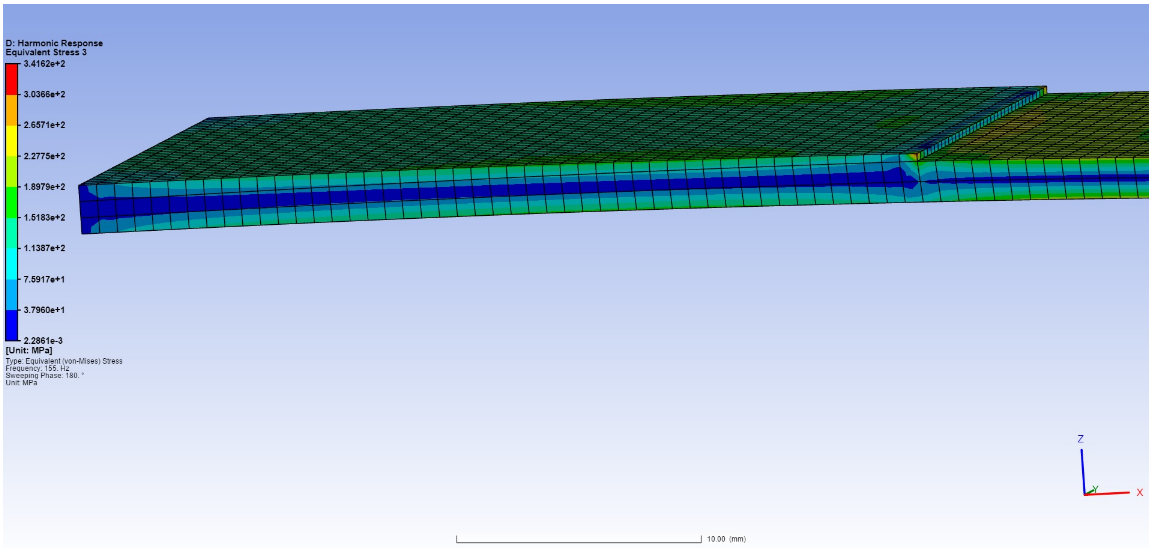

Figure 5.5: Stress Distribution on Specimen 0-90

Table 5.4: Extracted Stress from Specimen UD and Specimen 0-90

Specimen UD		Specimen 0-90	
Normal Stress (MPa)	Shear Stress (MPa)	Normal Stress (MPa)	Shear Stress (MPa)
107	54	115	64

Case of crack Feature on specimen 0-90

Since specimen 0-90 has a uniform delamination, the same size of crack occurred in the experiment is implemented in the model. The 3D model is exactly the same as previous, only with the addition of feature of crack. The crack thickness is 7.5 µm, which is 0.3 of the size of the seeded polymide. The thickness is approximated to match with the actual size of crack, of which is under the size of crack initiator thickness, 25 µm. The crack initiator reference can be seen in Figure 5.6. The crack width is as the component width because its delamination.

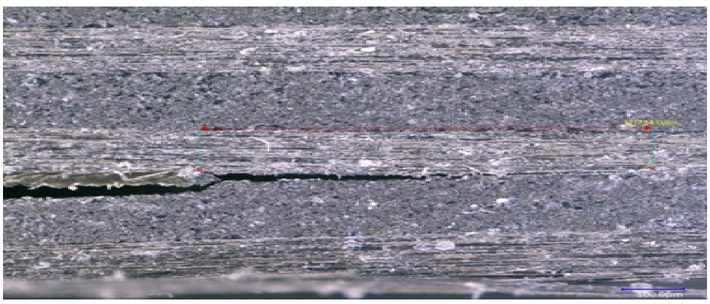

Figure 5.6: Micrograph of specimen 0-90

The simulation is run for each size of crack, and repeated until it reaches the longest crack size. The simulated crack are presented in Figure 5.7. The stress extracted from each size of crack will later be used to obtain strain energy release rate in the next Section 5.2.

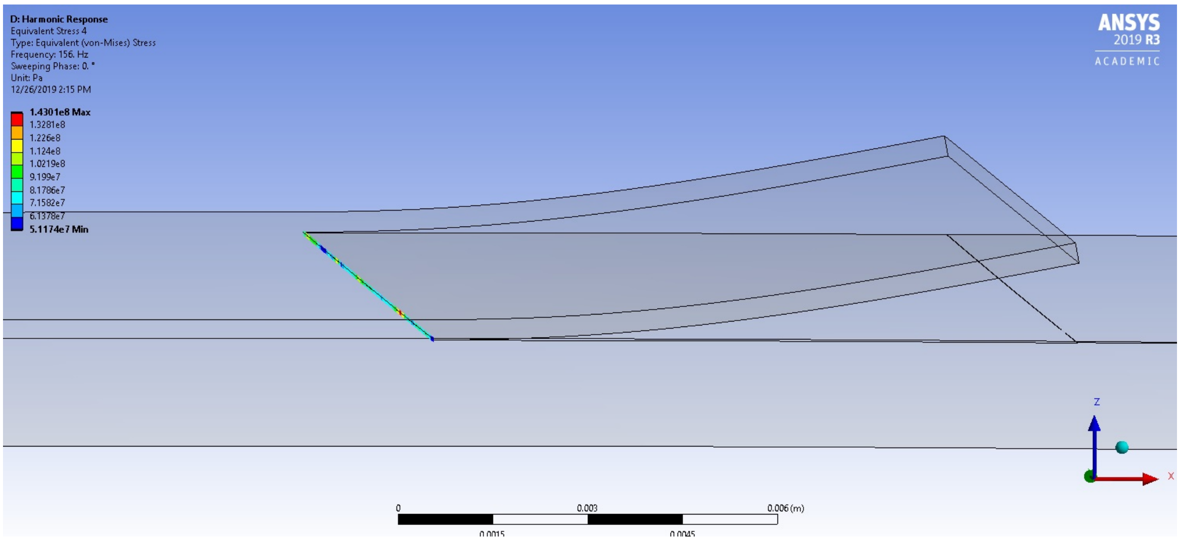

(a)

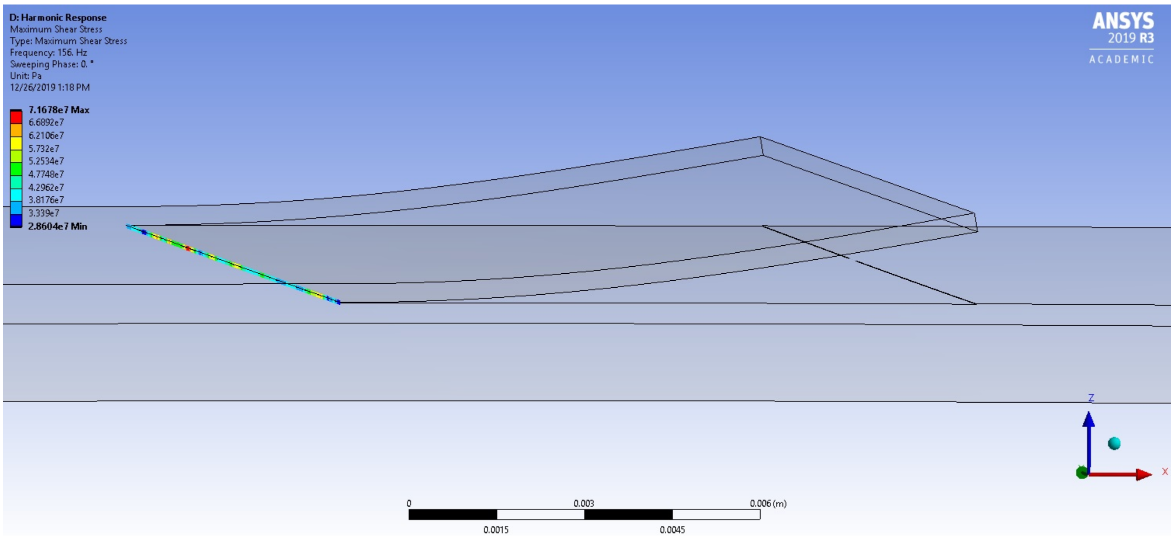

(b)

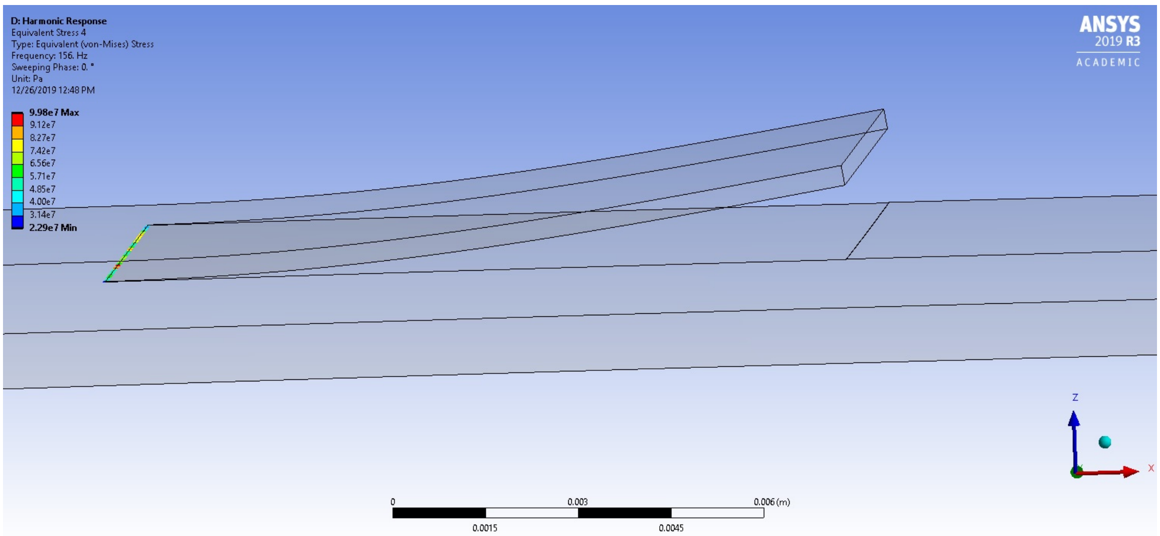

(c)

Figure 5.7: Steady-state dynamics imposed on specimen 0-90 (a) Crack 0.19 mm (b) Crack 0.94 mm (c) Crack 1.98 mm

The sensitivity of the resonance frequency reduction to the reduction of stiffness due to the cracks size is evaluated. The reduction of resonance frequency from the model, and from experiment are shown in the Table 5.5. The results from model and experiment are quite close which shows the stiffness reduction of the model is held valid with the experiment.

Table 5.5: Resonant frequency reduction caused by the crack from the experiment and model of specimen 0-90

Crack	Resonance Reduction (Hz)		Normal	Shear
Length (mm)	Model	Experiment	Stress (MPa)	Stress (MPa)
0.19	5.46	5.48	143	81.4
0.94	5.91	5.82	128.7	71.7
1.98	6.53	6.2	99.8	52

5.2 Crack Growth Law

As a delamination grows at a constant vibration loading, the cyclic G changes. Therefore, the delamination growth rate changes. Eventhough, Rans et al. [32] have discussed, that if one wishes to maintain the same similitude basis as Paris et al., (i.e. ΔK) then $\Delta\sqrt{G}$ should be selected as similitude parameter. Nevertheless, the most used similitude parameters for crack growth in composites are G_{max}, and ΔG. G_{max} and ΔG relate to the maximum crack tip stress, and to the externally applied cyclic work. In the vibration fatigue testing, since $R =$ -1, both similitude parameters result in the same proportional value. It is well explained in Matsubara et.al [33] for further details. This understanding is then used to obtain plots of G_{Imax} and G_{IImax} versus da/dN.

For the mode-mixity, Russell et.al [34] explained that the SERR for mode II in a fully reversed cycle has two peaks instead of one, hence the energy spent in each cycle to open a crack at $R =$ -1 is twice the energy spent in each cycle to open a crack at $R =$ 0 [34]. Magi [5] pointed out that regardless of the reverse loading condition in vibration fatigue test, mode II is at $R =$ -1, whilst mode I is at $R =$ 0. Furthermore, Matsubara et.al. [33] used the relationship in Equation 5.1. Whereas, each G is calculated using Equation 2.3, and Equation 2.4.

$$\Delta G = G_{\text{IImax}} \cdot (1 - R)^2 \tag{5.1}$$

Hence, The Paris's law is read as follows,

$$\frac{\mathrm{d}a}{\mathrm{d}N} = C\left(G_{\text{Imax}} + 4G_{\text{IImax}}\right)^m \tag{5.2}$$

In his work, Magi [5] relates the mode-mixity with its fracture toughness. However, worth to remember that it is just a way to understand the material properties of the studied composite. In this work, both Equations 5.2, and Equation 5.3 give close number of C, and m.

Nevertheless, Equation 5.2 is preferred, since the former gives dimensionless value.

$$\frac{\mathrm{d}a}{\mathrm{d}N} = C\left(\frac{G_{\text{Imax}}}{G_{\text{IIc}}} + \frac{4G_{\text{IImax}}}{G_{\text{IIc}}}\right)^{m} \tag{5.3}$$

The results for vibration fatigue (Mode I and Mode II) for the UD component is shown in Figure 5.8. The Y axis, which is the delamination growth rate is the experimental result. Whereas, X axis is the result of simulation that has been established in section 5.1. The red line, which is in power law, are obtained by least squares fit of the obtained data. The slope gives material coefficient, exponent m=0.8499 and c=1.446e-08.

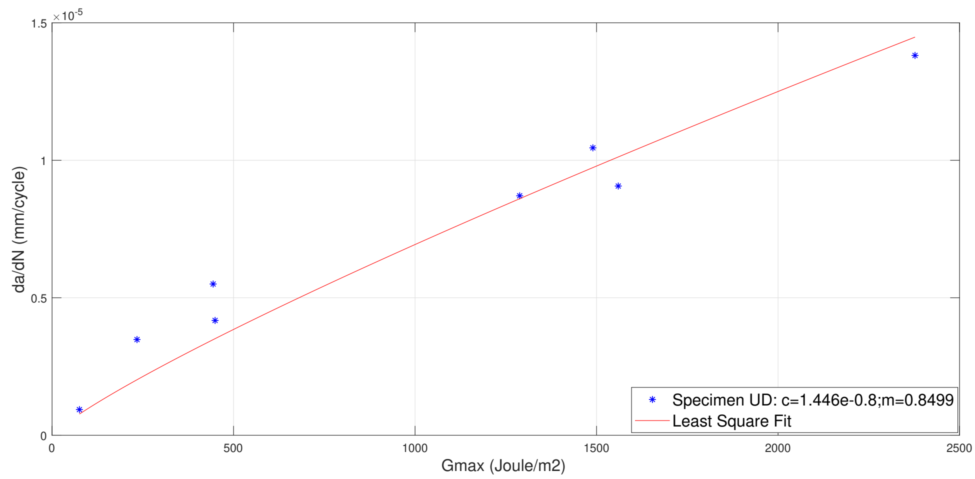

Figure 5.8: Propagation Rate Specimen UD from pristine model

The results for vibration fatigue (Mode I and Mode II) for specimen 0-90 is shown in Figure 5.9. Both strain energy release rate of pristine and of crack case are shown. The material coefficient results, which is m=0.6265 and c=1.378e-08, are having close value with the result of specimen UD. With the case of crack model, each of stress is extracted from the crack tip front. The Y axis, which is the delamination growth rate is the experimental result. Whereas, the X axis is the result of model that has been established in section 5.1.

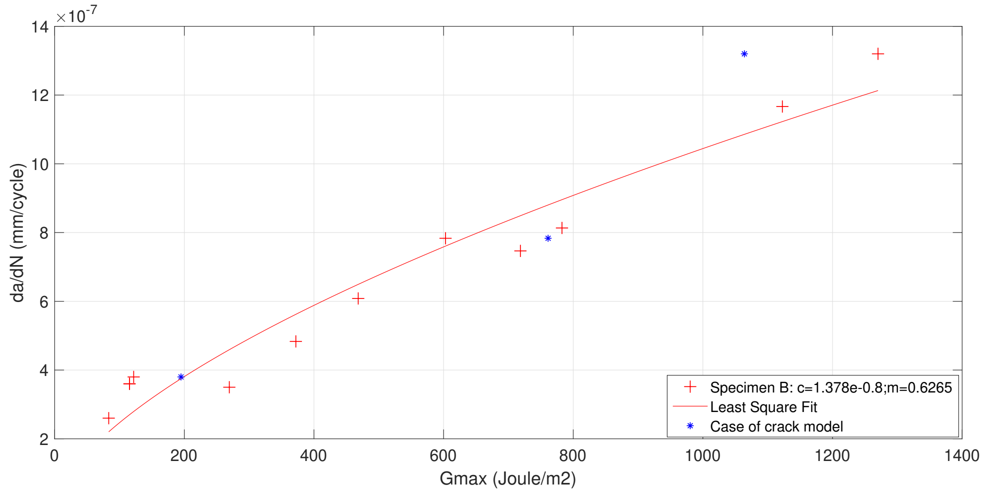

Figure 5.9: Propagation Rate Specimen 0-90 from Pristine model and Case of Crack Model

Both Figure 5.8 and Figure 5.9 show a good agreement. The R-square for both specimens are 0.9205 and 0.9384 respectively. The acquired relationship gives an understanding how strain energy release rate influence the crack growth rate in ply-drops specimen in the case of vibration loading. Specimen UD has a steeper curve which is aligned with its higher crack growth rate. Meanwhile, specimen 0-90 shows a less steeper slope while having higher resistance to delamination indicated from the initial SERR that creates the early initial crack.

Table 5.6: Comparison of exponent m [8]

Derivation	**Exponent m**		**Remark**
	Mode I	**Mode II**	
Current study (Denny's)	0.8752 (R=-1)		Specimen UD
Current study (Denny's)	0.6265 (R=-1)		Specimen 0-90
Literature			
Roderick H. Martin	6.14 (R=0.1)	3.65 (R=0.1)/ 5.34 (R=0.5	Quasi Static Load
Mall, Yun, and Kochhar, 1987	4.8 (R=0.1)	3.66 (R=0.1)	Quasi Static Load
Prel, Davies, Benzeggagh, and de Charentenay 1987	10.5 (R=0.1)	2 (R=-1)	Quasi Static Load
Russel, and Street, 1987	3 (R=0.1)	2.02 (R=-1)	Quasi Static Load

When compared with the results from the quasi static loading, as in Tabel 5.6, the results are quite scatter, except with the result from Russel and Street, with the same loading ratio. Nevertheless, Paris Law could not explain clearly the influence of mode-mix, loading ratio (R), and temperature [35]. Pascoe [35] clearly explained that all these studies have attempted to deal with these factors through modifications of the basic equations, but no fundamental explanation of the underlying phenomena. There is no proven model for general crack growth predictions. Nevertheless, these results enrich the perspective of the fatigue crack growth (FCG), since the results are from high cyclic loading.

Chapter 6

Conclusions and Recommendation

6.1 Conclusions

The work started from designing and manufacturing the fit ply-drop specimen. The discovered specimens, specimen UD and specimen 0-90 are brought to vibration fatigue test. The effect of high cycle fatigue is evaluated through its stiffness degradation, and dynamics parameters, and microscope to understand its structural performance. Ultimately, the work is then extended on the derivation of crack growth law. Therefore, each research questions was answered separately in the previous chapters. Therefore, conclusion can be summarized as follows,

1. Thermoplastic-based composite, in this case TC 1320 PEKK, is found highly resistant to fatigue. For ply-drops testing specimen, it needs pre-existence crack as crack initiator. The crack propagation rate has been explained in Chapter 4.
2. The effect of crack to dynamic parameters has been explained and employed to monitor crack initiation, which is described in chapter 4. Base acceleration trace and phase response shift can clearly explain when the crack is initiating, and start propagating. The phase response shift is found more sensitive than base acceleration trace. The three events from initiation until propagation has already been established.
3. Paris law has been derived from ply-drop based thermoplastic. The good agreement on the value of variable m found between different stacking sequence, specimen UD, and 0-90, which means it reflects the characteristic of identical material properties of both composites. The difference is the result of different stacking sequence, which gives different propagation rate.

6.2 Recommendation and Future Work

This work indeed provides structural integrity performance of composite through vibration fatigue loading in a dynamics environment. There is still further in-depth analysis to be made resulting in a more accurate structural performance of composite, specifically material properties C, and m, by incorporating various elements as follows:

1. Evaluation of delamination by employing C-Scan can take into account a more accurate length and severity of the delamination. Accurate length of crack results in a better derivation of exponent m. Determining the dimension of delamination through C-Scan is proposed for future researches.

2. The future challenge for a thorough understanding of thermoplastic under fatigue conditions lies in combining Paris Law from mechanical testing, which is of quasi-static load and vibration testing, which is of dynamic load. It is now known that the vibration testing operates in capturing the a portion regime of Paris Law. And, the propagation happens rapidly. Meanwhile, mechanical testing through ASTM D5228/ASTM D6115 can cover up to entire regime of propagation. Combining these two different condition will determine the performance of the composite accurately.

3. The self-generated heating due to the low thermal conductivity of the composite material is likely to appear at elevated loading frequencies. To evaluate specimen self-heat generation, specimen temperature evolution should be taken into account with the use of a thermal camera near the crack tip, as well as, on the entire body of specimen.

Bibliography

[1] A. Mukherjee and B. Varughese, "Design guidelines for ply drop-off in laminated composite structures," *Composites Part B: Engineering*, vol. 32, no. 2, pp. 153–164, 2001.

[2] M. Holmes, "Global carbon fibre market remains on upward trend," *Reinforced Plastics*, vol. 58, no. 6, pp. 38–45, 2014.

[3] K. Reifsnider, "Fatigue behavior of composite materials," *International Journal of Fracture*, vol. 16, no. 6, pp. 563–583, 1980.

[4] M. Alvarez, "Characterization of impact damage in composite laminates," The Aeron Research Institute of Sweden, Bromma, Tech. Rep., 1998.

[5] F. Magi, "Vibration fatigue testing for identification of damage initiation in composites," Ph.D. dissertation, University of Bristol, 2016.

[6] R. Ritchie, "Near-threshold fatigue-crack propagation in steels," *International Metals Reviews*, vol. 24, no. 1, pp. 205–230, 1979.

[7] F. Magi, D. Di Maio, and I. Sever, "Damage initiation and structural degradation through resonance vibration: Application to composite laminates in fatigue," *Composites Science and Technology*, vol. 132, pp. 47–56, 2016.

[8] R. H. Martin and G. B. Murri, "Characterization of mode i and mode ii delamination growth and thresholds in as4/peek composites," in *Composite materials: testing and design (Ninth Volume)*. ASTM International, 1990.

[9] S. Mazumdar, *Composites manufacturing: materials, product, and process engineering*. CrC press, 2001.

[10] Y. J. Prel, P. Davies, M. L. Benzeggagh, and F.-X. de Charentenay, "Mode i and mode ii delamination of thermosetting and thermoplastic composites," in *Composite Materials: Fatigue and Fracture, Second Volume*. ASTM International, 1989.

[11] D. Carlile and D. Leach, "Damage and notch sensitivity of graphite/peek composite." in *20/20 VISION IN MATERIALS FOR 2000- NAT. SAMPE TECH. CONF. SER., 1983,*, vol. 15, 1983, pp. 82–93.

[12] K. Boller, "Fatigue fundamentals for composite materials," in *Composite materials: testing and design*. ASTM International, 1969.

[13] A. Lystrup and T. L. Andersen, “Autoclave consolidation of fibre composites with a high temperature thermoplastic matrix,” *Journal of Materials Processing Technology*, vol. 77, no. 1-3, pp. 80–85, 1998.

[14] D. Cairns, J. Mandell, M. Scott, and J. Maccagnano, “Design and manufacturing considerations for ply drops in composite structures,” *Composites Part B: Engineering*, vol. 30, no. 5, pp. 523–534, 1999.

[15] J. Bailie, R. Ley, and A. Pasricha, “A summary and review of composite laminate design guidelines,” *Langley RC, Hampton*, 1997.

[16] D. Di Maio, F. Magi, and I. Sever, “Damage monitoring of composite components under vibration fatigue using scanning laser doppler vibrometer,” *Experimental Mechanics*, vol. 58, no. 3, pp. 499–514, 2018.

[17] D. Dew-Hughes and J. Way, “Fatigue of fibre—reinforced plastics: a review,” *Composites*, vol. 4, no. 4, pp. 167–173, 1973.

[18] A. A. Griffith, “Vi. the phenomena of rupture and flow in solids,” *Philosophical transactions of the royal society of london. Series A, containing papers of a mathematical or physical character*, vol. 221, no. 582-593, pp. 163–198, 1921.

[19] G. R. Irwin, “Analysis of stresses and strains near the end of a crack traversing a plate,” 1997.

[20] P. C. Paris, “A rational analytic theory of fatigue,” *The trend in engineering*, vol. 13, p. 9, 1961.

[21] W. Clark and S. Hudak, “Variability in fatigue crack growth rate testing,” *Journal of Testing and Evaluation*, vol. 3, no. 6, pp. 454–476, 1975.

[22] J. A. Pascoe, R. C. Alderliesten, and R. Benedictus, “Methods for the prediction of fatigue delamination growth in composites and adhesive bonds–a critical review,” *Engineering Fracture Mechanics*, vol. 112, pp. 72–96, 2013.

[23] B. Lazan, A. Gannett, P. Kirmser, J. Klumpp, and J. Brown, “Dynamic testing of materials and structures with a new resonance-vibration exciter and controller,” MINNESOTA UNIV MINNEAPOLIS, Tech. Rep., 1952.

[24] D. Di Maio and F. Magi, “Development of testing methods for endurance trials of composites components,” *Journal of Composite Materials*, vol. 49, no. 24, pp. 2977–2991, 2015.

[25] O. Kovářík, P. Haušild, J. Čapek, J. Medřickỳ, J. Siegl, R. Mušálek, Z. Pala, N. Curry, and S. Björklund, “Resonance bending fatigue testing with simultaneous damping measurement and its application on layered coatings,” *International Journal of Fatigue*, vol. 82, pp. 300–309, 2016.

[26] Y.-J. Kee, T.-J. Kim, S.-W. Moon, and J.-H. Han, “Resonant fatigue testing of full-scale helicopter blades from composite laminated materials,” in *Proceedings of the Korean Society for Noise and Vibration Engineering Conference*. The Korean Society for Noise and Vibration Engineering, 2010, pp. 82–83.

[27] S.-H. Han, D.-G. An, S.-J. Kwak, and K.-W. Kang, “Vibration fatigue analysis for multi-point spot-welded joints based on frequency response changes due to fatigue damage accumulation,” *International Journal of Fatigue*, vol. 48, pp. 170–177, 2013.

[28] P. Lorenzino and A. Navarro, “The variation of resonance frequency in fatigue tests as a tool for in-situ identification of crack initiation and propagation, and for the determination of cracked areas,” *International Journal of Fatigue*, vol. 70, pp. 374–382, 2015.

[29] D. J. Ewins, *Modal testing: theory and practice*. Research studies press Letchworth, 1984, vol. 15.

[30] B. Harris, *Fatigue in composites: science and technology of the fatigue response of fibre-reinforced plastics*. Woodhead Publishing, 2003.

[31] Toray, “https://www.toraytac.com/resources/datasheets,” p. 3, 2019.

[32] C. Rans, R. Alderliesten, and R. Benedictus, “Misinterpreting the results: How similitude can improve our understanding of fatigue delamination growth,” *Composites Science and Technology*, vol. 71, no. 2, pp. 230–238, 2011.

[33] G. Matsubara, H. Ono, and K. Tanaka, “Mode ii fatigue crack growth from delamination in unidirectional tape and satin-woven fabric laminates of high strength gfrp,” *International Journal of Fatigue*, vol. 28, no. 10, pp. 1177–1186, 2006.

[34] A. J. Russell and K. N. Street, “The effect of matrix toughness on delamination: static and fatigue fracture under mode ii shear loading of graphite fiber composites,” in *Toughened composites*. ASTM International, 1987.

[35] J. Pascoe, “Characterisation of fatigue crack growth in adhesive bonds,” 2016.

Appendix A

A.1 Procedures of vacuum bagging

1. Place release film on top of the base plate for easy removal of the laminate.
2. Apply sealant tape to all the edges of the plate. Seal tape is 1-inch-wide rubbery material that sticks to both the mold and bagging material.
3. After placing the release film, place the prepared prepregs just on top of the film.
4. Place fabric cloths on all sides of the prepregs that serve as a bleeder.
5. Place release film on top of the prepreg stack.
6. Place fibres glass cloth, as breather, on top of the release film. The purpose of using the glass cloth is to absorb moisture and excess resin coming from the stack of prepregs.
7. The final layer is expendable polyamide (PA) film as a vacuum bag. This film is attached to sealant tape in such way cover the stacked prepregs.

A.2 Property of Specimen A and B

Property	Specimen A	Specimen B
Nodes	77646	77646
Elements	14245	14245
Mesh Metric	Element Quality	Element Quality
Min	0.696936081301615	0.696936081301615
Max	0.999034535354464	0.999034535354464
Average	0.977182991153758	0.977182991153761
Standard Deviation	4.69085828226485E-02	4.69085828225999E-02

Appendix B

Appendix B

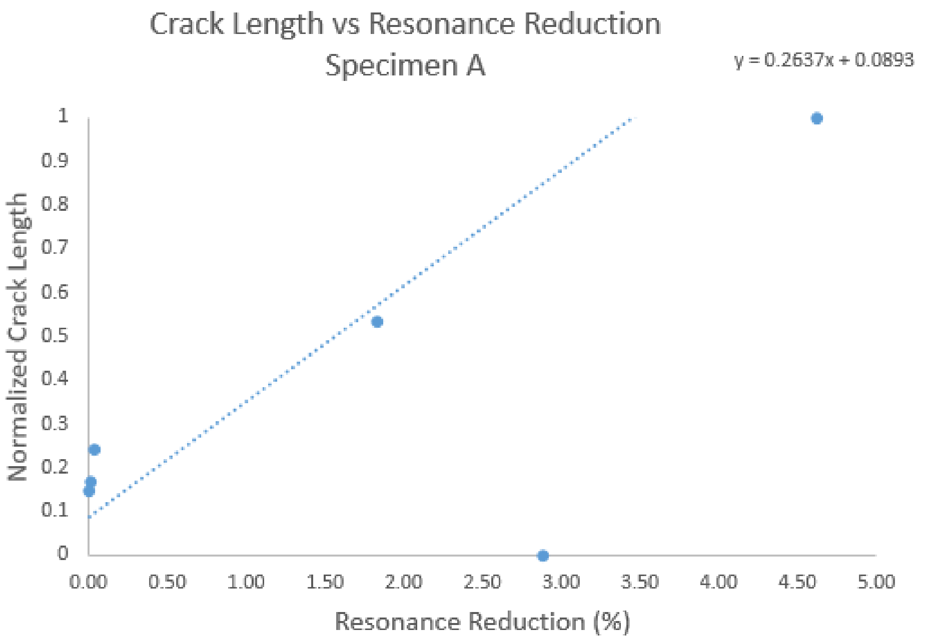

(a)

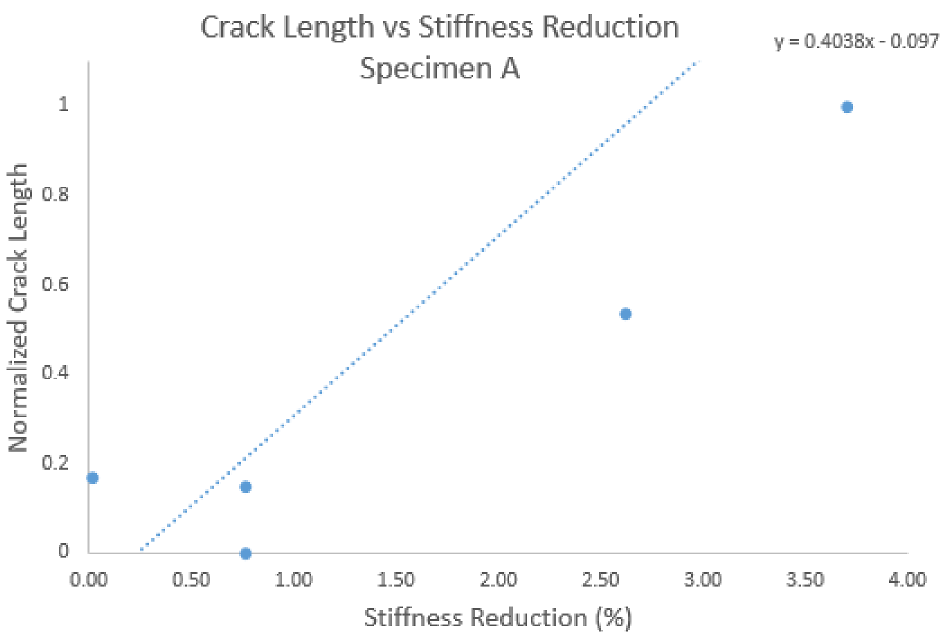

(b)

Appendix C

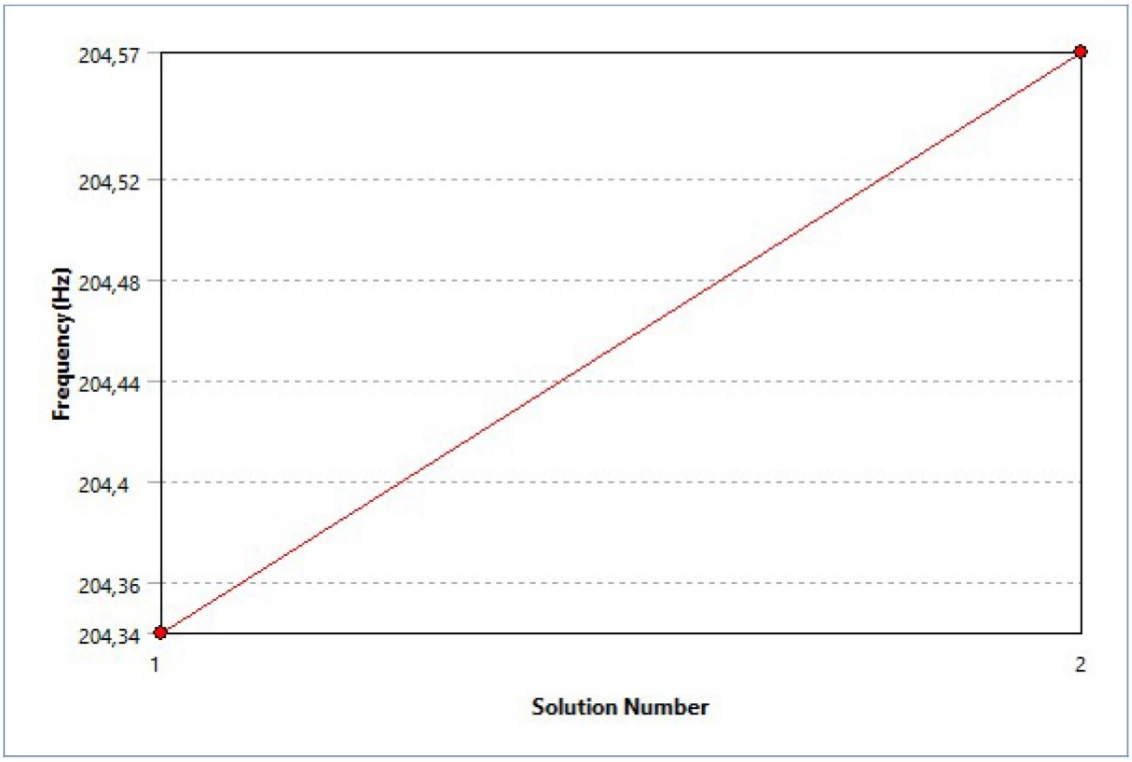

Model (C4) > Modal (C5) > Solution (C6) > Total Deformation 2 > Convergence

	Frequency(Hz)	Change (%)	Nodes	Elements
1	204,34		20853	3743
2	204,57	0,10909	102432	62181

Figure C.1: Convergence Modal Specimen UD

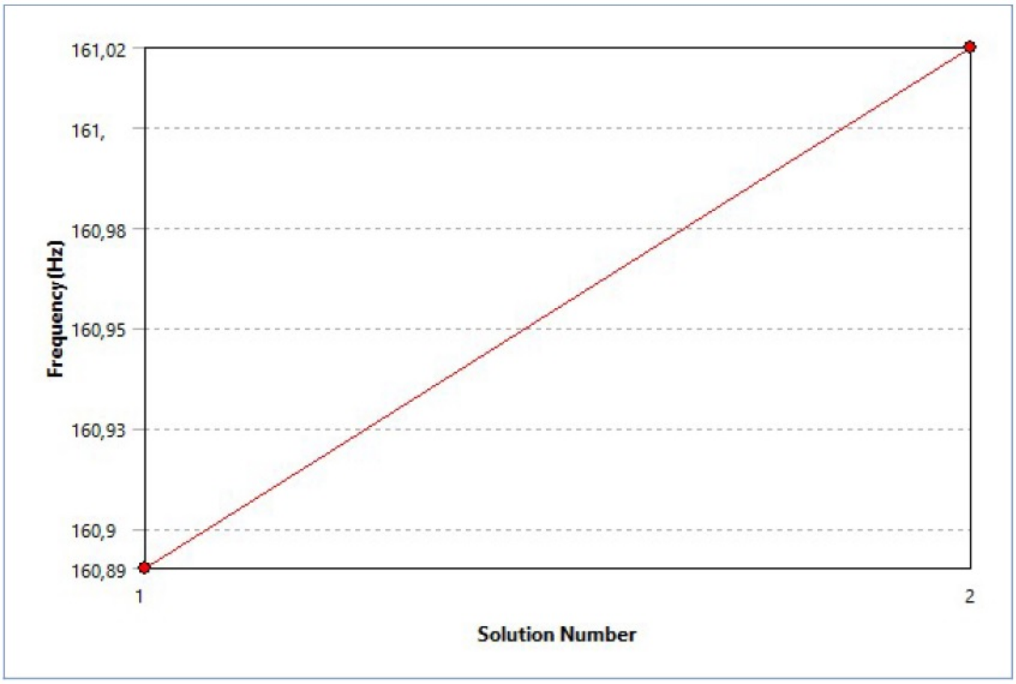

Model (C4) > Modal (C5) > Solution (C6) > Total Deformation 2 > Convergence

	Frequency(Hz)	Change (%)	Nodes	Elements
1	160,89		12878	1926
2	161,02	8,1366e-002	107499	64390

Figure C.2: Convergence Modal Specimen 0-90